Medizinische Fakultät
der
Universität Duisburg-Essen

Aus dem Institut für Anatomie

Granule Cell Raphes in the Developing Mouse Cerebellum

I n a u g u r a l – D i s s e r t a t i o n
zur
Erlangung des Doktorgrades der Medizin
durch die Medizinische Fakultät
der Universität Essen

Vorgelegt von
Robert Stefan Luckner
aus Bytom (Beuthen), Polen
2007

Dekan: Herr Univ.-Prof. Dr. K.-H. Jöckel
1. Gutachter: Herr Univ.-Prof. Dr. D. Büsselberg
2. Gutachter: Herr Univ.-Prof. Dr. Dr. Chr. Redies, Jena

Tag der mündlichen Prüfung: 11. März 2008

Teile dieser Arbeit wurden veröffentlicht in:

Originalveröffentlichungen:

R. Luckner, K. Obst-Pernberg, S. Hirano, S.T. Suzuki and C. Redies
Granule cell raphes in the developing mouse cerebellum
Cell and Tissue Research (2001) 303:159-172

C. Redies, R. Luckner and K. Arndt
Granule cell raphes in the cerebellar cortex of chicken and mouse
Brain Research Bulletin (2002) 57:341-343

Kongressbeiträge:

R. Luckner, K. Obst-Pernberg und C. Redies
Granule Cell Raphe in the Developing Cerebellar Cortex of the Mouse
Posterveröffentlichung auf der 16. Arbeitstagung der Anatomischen Gesellschaft, Würzburg, 29.09. – 01.10.1999

C. Redies, R. Luckner and K. Arndt
Granule cell raphes: A common and basic scheme of parasagittal organization in the cerebellar cortex of chicken and mouse
Abstract für die 3rd European Conference on Comparative Neurobiology, Murcia, Spain (19-21 April 2001)

R. Luckner, K. Obst-Pernberg and C. Redies
Granule Cell Raphe in the Developing Cerebellar Cortex of the Mouse
Posterveröffentlichung auf dem 1. Forschungstag der medizinischen Fakultät der Universität Essen, 2002

LIST OF CONTENTS

1. INTRODUCTION

1.1 Granule Cell Raphe

In many vertebrates, the cerebellar cortex shows a striking parasagittal modular organization (for reviews, see Hawkes and Mascher, 1994; Herrup and Kuemerle, 1997; Oberdick et al., 1998; Larouche and Hawkes, 2006) which is reflected not only in its afferent and efferent connectivity (Groenewegen and Voogd, 1976; Arends and Zeigler, 1991; Wassef et al., 1992; Voogd and Glickstein, 1998; Sugihara, 2006) but also in the expression of various molecular markers, such as gene regulatory proteins (Millen et al., 1995; Lin and Cepko 1998), cell adhesion molecules (Arndt and Redies, 1996; Chédotal et al., 1996; Fushimi et al., 1997; Korematsu and Redies, 1997; Suzuki et al., 1997; Arndt et al., 1998; for review, see Redies, 2000; Marzban et al., 2003) and other types of molecules (Wassef et al., 1985; Eisenman and Hawkes, 1993; Oberdick et al., 1993; Sarna et al., 2006). In the mouse, the medio-lateral compartmentalization starts with the birth of Purkinje cells between E10.5 and E12.5 (Hashimoto and Mikoshiba, 2003)

It is generally agreed upon in the literature that these molecules can be grouped into markers that reflect an “early-onset” parasagittal banding pattern in the developing (perinatal) cerebellum and those that reflect a “late-onset” banding pattern, which sets in later in development and persists in the mature cerebellum (for review, see Herrup and Kuemerle, 1997). The relationship between these two types of patterns has remained elusive, because there is, in general, no or little temporal overlap between the expression of early-onset markers and late-onset markers in the parasagittal compartments. While some authors have speculated that the two types of pattern are related to one another (Herrup and Kuemerle, 1997), experimental evidence shows that the two types of pattern are differentially affected by the ectopic expression of the gene regulatory molecule En2 (Baader et al., 1999).

Following publications of my own data (Luckner et al., 2001) neurogranin, a member of the calpacitin protei0n family, has been described as a marker bridging the temporal gap between the early-onset pattern and the late-onset pattern (Larouche et al., 2006). Neurogranin is endogenously produced by the Purkinje cells from the embryonic day E15 until post natal day P20.

The precise number of mediolateral compartments is also a matter of controversy (for review, see Oberdick et al., 1998). On the one hand, it is clear that a vast number of unique domains can be defined based on their expression of combinations of the parasagittal markers available to date. On the other hand, heterogeneities and borders of expression are often found to coincide for several different markers. Based on an analysis

of such common borders, it has been proposed that there exist a set of about six to eight distinct mediolateral compartments (Herrup and Kuemerle, 1997).

It was shown by Arndt et al. (1998) that, at intermediate stages of development, the cerebellar cortex of chicken contains parasagittal ribbons of migrating granule cells and interneurons that express specific cadherins. These ribbons of migrating cells extend from the external granular layer through the developing molecular layer into the internal granular layer. It has been proposed (Fushimi et al., 1997; Arndt et al., 1998) that the ribbons are identical to the "granule cells raphes" first described on histological grounds by Feirabend (1983; see Fig.1) between about 9 and 15 days of incubation in chicken.

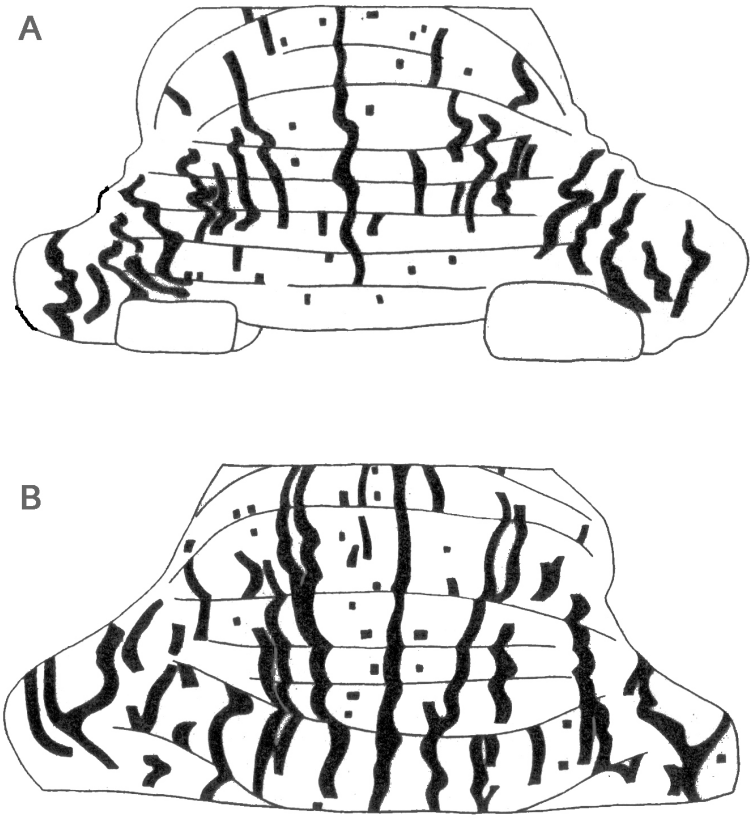

Fig. 1A-B Granule cell raphes in the avian cerebellum. An anterior (**A**) and posterior (**B**) view. Reconstruction of a 14 days old embryo (Hamburger and Hamilton stage 39). Reproduced from Feierabend (1983).

The granule cell raphes separate parasagittal segments of Purkinje cells, which differentially express cadherins (Arndt et al., 1998). This complementary arrangement of granule cell raphes and Purkinje cell segments has been confirmed by Lin and Cepko (1998) who showed that several other molecules also exhibit expression domains which sharply coincide with the pattern of granule cell raphes.

In the present study, I will show that granule cell raphes are also found in the cerebellar cortex of the mouse at intermediate stages of development. Like in the chicken, these granule cell raphes show a higher cell density than the surrounding molecular layer and they are frequently found at the borders of cadherin-expressing Purkinje cell clusters. A study by Karam at al. (2001) has subsequently confirmed the presence of granule cell raphes in mice and primates.

The term ‘raphe’ has been previously used by Korneliussen (1967, 1968) for cell-poor (‘medullary’) structures observed between longitudinal zones of developing cerebellar cortex and deep cerebellar nuclei of several mammalian species. These structures are different from the cell-dense granule cell raphes described in the present work.

1.2 The Gross Anatomy of the Mammalian Cerebellum

The mammalian cerebellum originates mostly from the neural tissue in the rostral metencephalon. In vertebrates, the cerebellum occupies a position in the occipital part of the skull behind the rhombencephalon; it forms the roof of the fourth ventricle.

Like the cerebrum, the cerebellum is composed of several parts, which differ in their appearance during evolution (Trepel, 1995), in their connectivity (Wassef et al., 1992; Voogd et al., 1998), and in their gene expression (Wassef et al., 1985; Oberdick et al., 1998). The main known function of the cerebellum is the coordination and modulation of movements. In addition some studies indicate a crucial role of the cerebellum in the control of mental behavior (e.g. Ito, 1993). To accomplish this function, the cerebellum receives afferents from the pons, the spinal cord and the brainstem, and here, in particular, from the vestibular nuclei, the inferior olive and the reticular formation.

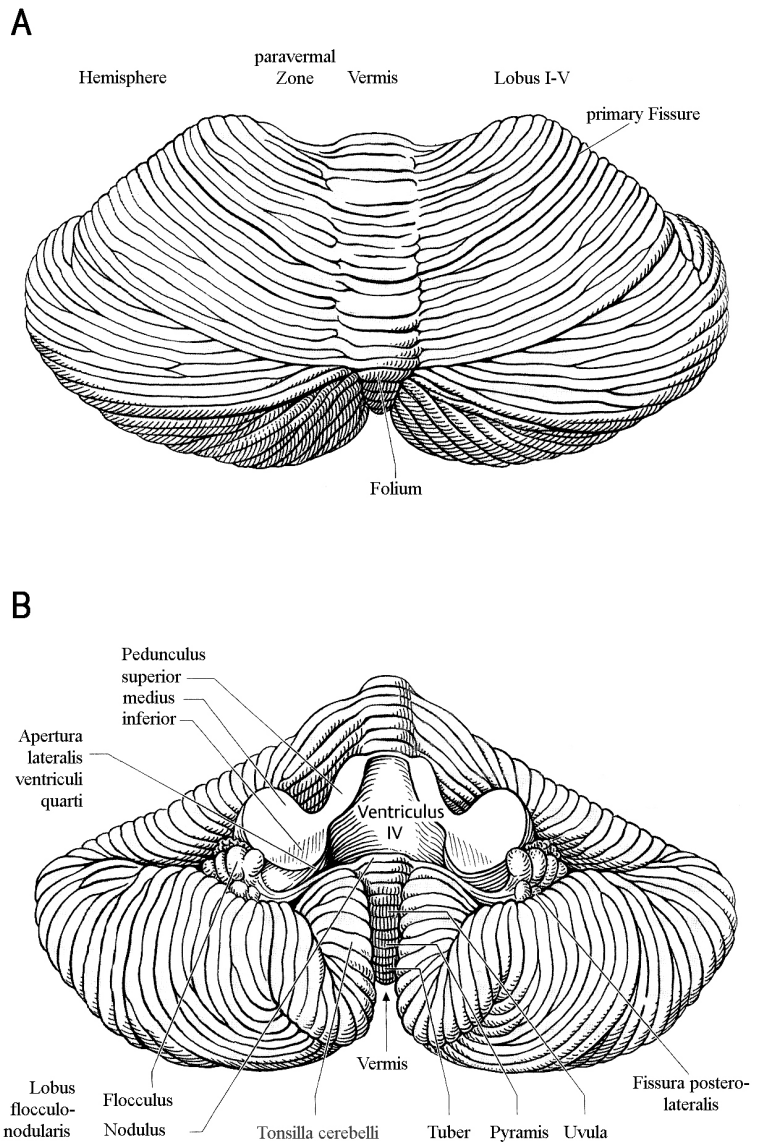

Fig. 2A-B The gross anatomy of the human cerebellum (schematic drawing). View from rostral (**A**) and caudal (**B**). Modified after Bähr et al. (2003).

The lobus flocculo-nodularis, the evolutionary oldest part, is located in the caudal pole of the cerebellum and is closely related to the vestibular system. This portion of the cerebellum is called arch cerebellum due to its early phylogenetic origin. The so-called vermis, the middle part of the cerebellum, gets most of its afferent input from the spinal cord. Together with the paravermal zone, it is called spinocerebellum. In phylogenetic age, it is thought to be intermediate between the arch cerebellum and the neocerebellum. The neocerebellum consists of two hemispheres, which represent, in evolution, the youngest and largest part of the cerebellum (see Fig. 2, Trepel, 1995; Altman and Bayer, 1997). The hemispheres receive most of their afferents from the pons. They have increased

enormously in volume, in parallel with the upright posture of vertebrates (Voogd and Glickstein, 1998).

The neuronal tracts which connect the cerebellum with the brainstem run through three cerebellar peduncles (superior, medial and inferior cerebellar peduncle) (Trepel, 1995).

The cerebellar cortex has a foliated appearance, due to its large surface and its development in a relatively small area in the posterior fossa of the skull. The typical layered architecture of the cerebellum continues in the depth of the foliated cortex. Several folia together form a cerebellar lobule. The cerebellum of mammals is divided into ten lobules (Larsell, 1952), usually denoted by the Roman numerals I-X.

Deep transverse fissures form anatomical boundaries between the lobules at given positions. The most prominent fissures are: the primary fissure in the rostral part of the cerebellum which separates lobules I-V from lobules VI-VIII, and the secondary fissure between lobules VIII and IX. The nodulus, also known as lobule X, is divided from the rest of the cerebellum by the posterolateral fissure (see Fig. 2; Trepel, 1995; Altman and Bayer, 1997).

1.3 The Cells of the Cerebellum

The cortex of the adult cerebellum consists of three layers. From the inside to the outside, above the inner white matter, the internal granule cell layer is found, followed by a single row of Purkinje cells and the molecular layer (see Fig. 3). All these layers are built by five types of neurons: the granule cells, the Purkinje cells, the Golgi cells, the small stellate cells and the basket cells. The last three types of neurons are inhibitory interneurons (Trepel, 1995).

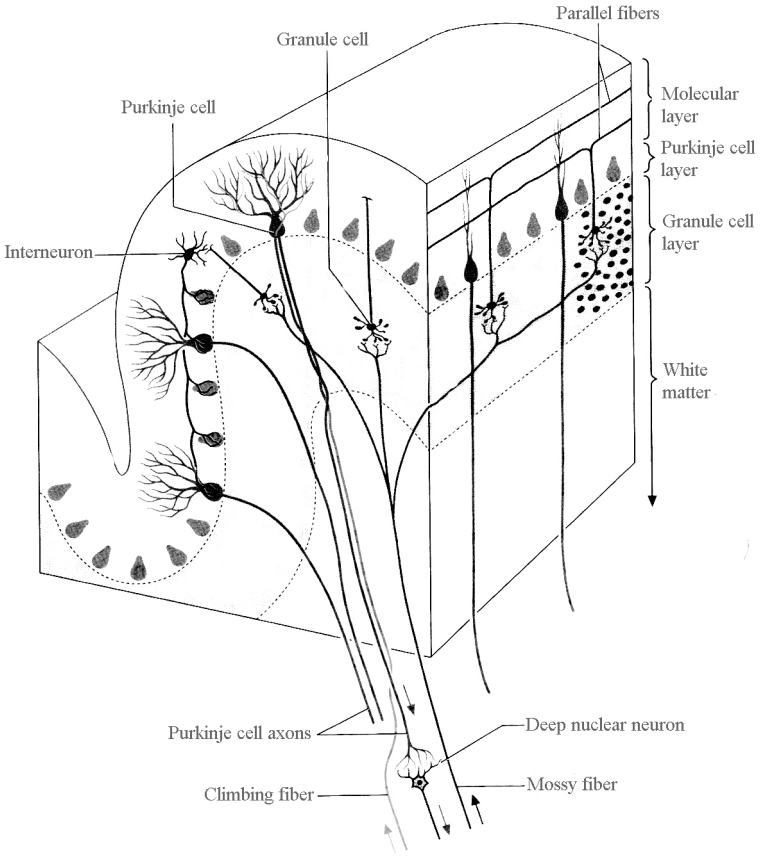

Fig. 3 Cellular organization of the cerebellar cortex. Schematic drawing modified after Bähr et al. (2003).

Most cells of the cerebellum arise from a germinal matrix region in the rostral metencephalon (Altman and Bayer, 1997; Goldowitz and Hamre, 1998; Larouche and Hawkes, 2006). Mathis et al. (1997) have shown that all cerebellar neurons, with the exception of the granular cells, are clonally related. Around embryonic days E9-12 in the mouse, neurons leave the ventricular zone to build the deep cerebellar nuclei. They are followed by the generation of Purkinje cells, which build a temporary plate-like structure in the cerebellar cortex. At the time when the deep nuclei and Purkinje cells have stopped dividing (E10-13), the external granular layer (EGL) at the surface of the cerebellar cortex appears. This germinative layer generates the granular cells. During their differentiation, interneurons migrate from the ventricular zone into the cerebellar cortex, e.g. into the molecular layer. In parallel with the large increase of neurons and glial cells in the cerebellum, the volume of the cerebellum increases. The external form of the cerebellum transforms from a smooth surface into a surface with deep fissures and the so-called folia (Altman and Bayer, 1997; Goldowitz and Hamre, 1998).

1.3.1 Granule cells

The granule cells are glutamatergic neurons, that origin from the upper rhombic lip (Larouche and Hawkes, 2006). This population represents the most numerous of all neurons in the cerebellum (Trepel, 1995; Voogd and Glickstein, 1998). In the adult cerebellum, the granule cell layer assumes a position in the inner part of the cerebellar cortex (Trepel, 1995). The early granule cells do not migrate from the ventricular matrix in an inside/out direction, as is usually the case, e.g. for the cells in the cerebral cortex. In the developing cerebellum, the granular precursor cells migrate from the metencephalon into the upper rhombencephalic lip that later transforms into the cerebellum. Here, they first form the external granular layer. After the differentiation from neuroblasts into granule cells, the postmitotic cells migrate through the Purkinje cell layer toward the internal granular layer (outside/in direction). During this migration, the granule cells send out bifurcated unmyelinated axons (parallel fibers) to the dendrites of interneurons and Purkinje cells in the superficial molecular layer. Mossy fibers arising from many different sources of the brainstem and from the spinal cord make synaptic connections with the dendrites of granular cells (Goldowitz and Hamre, 1998; Voogd and Glickstein, 1998).

1.3.2 Purkinje cells

The largest cells of the cerebellum are the GABAergic Purkinje cells. In the mature cerebellum, they form a single cell layer at the border between the molecular layer and the granular cell layer. Parallel fibers of the granule cells connect to the distal parts of the dendrite trees of the Purkinje cells in the molecular layer, which are orientated perpendicularly to the parallel fibers. In the proximal part, close to the cell body, climbing fibers from neurons in the inferior olivary nucleus reach the branches of the Purkinje cell dendrites. The axons of the Purkinje cells are the sole efferents of the cerebellar cortex. They have direct synaptic connections to the deep nuclei of the cerebellum and to some nuclei of the brainstem, e.g. the vestibular nuclei (Trepel, 1995; Altman and Bayer, 1997; Voogd and Glickstein, 1998).

1.3.3 Interneurons

Golgi cells, stellate cells and basket cells act as inhibitory interneurons mostly in the molecular layer of the cerebellar cortex. The Golgi cells differ from the stellate/basket cells in their localization, connections to other cells, morphology and biochemical characteristics (Voogd and Glickstein, 1998). Parallel fibers and collaterals of Purkinje cell axons terminate at the surface of the Golgi cells (Trepel, 1995). In this way, the small

interneurons, which are GABA- and glycinergic, provide a feed-backward inhibition to the granule cells with their axons. The stellate/basket cells that are purely GABAergic make connections with the parallel fibers and the collaterals of the Purkinje cell axons as well, but their axons terminate at the dendrite branches or at the cell bodies of the Purkinje cells, respectively. They provide a feed-forwarded inhibition (Trepel, 1995).

1.3.4 Glial cells

As non-neuronal cell populations in the cerebellum, radial glial cells act as pathways for the migration of neuronal cells on their way to their final position in the cerebellar cortex. The radial glia guide the Purkinje cells and the granule cells from they origin in the ventricular matrix and the external granule cell layer, respectively (Rakic, 1971; Hatten, 1993; Sotelo 1994). The Bergmann glias are located with their cell bodies in the Purkinje cell layer and reach into the molecular layer with their palisade-like processes (Trepel, 1995).

These are the main types of neuronal and glial cells in the cortex of the cerebellum. All these cells have special functions in the complex network of the cerebellar neurons.

1.4 The Output and Input of the Cerebellum

The output from the cerebellar cortex is conveyed by the Purkinje cell axons; the input is carried by the mossy and climbing fibers. These fiber systems are organized in a parasagittal pattern. The Purkinje cell axons of each cerebellar cortical zone project to specific parts of the deep cerebellar nuclei or directly to the vestibular nuclei of the hindbrain. Their projection zones can be followed across several cerebellar lobules. In some cases they extend over the entire rostro-caudal axis of the cerebellum. In the other direction, climbing fibers from the subnuclei of the inferior olive or mossy fibers, which have their source in the brainstem or in the spinal cord, project to one or a pair of Purkinje cell zones, which share the same nucleus. These zones form compartments of Purkinje cells with their axons as the output and the climbing fibers and the mossy fibers as the input (Trepel, 1995; Voogd and Glickstein, 1998).

Several biochemical markers reveal this compartmentation of the developing or adult cerebellum at the molecular level (Millen et al., 1995; Lin and Cepko 1998; Oberdick et al, 1998). I will concentrate on two proteins: cadherins as an “early onset”, and zebrin II as a “late onset” marker (Eisenman and Hawkes 1993; Hawkes and Mascher 1994).

1.5 The Molecules of the Cerebellum

1.5.1 Cadherins

Calcium-dependent adhesion molecules, also known as cadherins, were discovered in the late 80ies of the last century by M. Takeichi and other groups. The members of the cadherin superfamily are cell surface glycoproteins. Most cadherins consist of three domains: an intracellular domain, a transmembrane domain and an extracellular domain. The extracellular domain is characterized by several cadherin repeats, which contain calcium-binding motifs. The members of the different subgroups of cadherins (e.g., classic type I and II cadherins, protocadherins, etc.; see below) differ in the number of the cadherin repeats (Suzuki 1996) and in the molecular structure of the cytoplasmic domain. Some investigators have shown that the extracellular repeats have a very close relation to the variable domain of immunoglobulins (Overduin et al. 1995; Shapiro et al. 1995).

Cadherins are cell surface glycoproteins that play a crucial role in the adhesion of the cells in a given tissue or in an organ. The adhesiveness of cadherins depends on the presence of calcium (Takeichi et al. 1981; Nakagawa et al. 1997). The cadherins bind to other cadherins in a homotypic manner (i.e., to the same cadherin subtype) or in some cases in a heterotypic manner (i.e., to another cadherin subtypes). In general, homotypic binding is stronger than heterotypic binding. In some special cases, binding to other molecules, such as to the intergrins, has also been observed (Cepek et al. 1994).

On the cytoplasmic side, cadherins bind to several types of molecules. Many cadherins are linked to the catenins. By binding catenins, cadherins become connected to the cytoskeleton. In addition, cadherins play an important role in signal transduction. Some signaling pathways, in which cadherins are involved, play a role in cell proliferation, migration, differentiation and apoptosis. Thus, the function of cadherins is to regulate morphogenesis of several tissues and organs.

The cadherins described first are the type I classic cadherins. This subfamily of cadherins is named after the tissues they were discovered in, like N-cadherin (= neural cadherin), R-cadherin (= retinal cadherin), E-cadherin (= epithelial cadherin) and P-cadherin (= placental cadherin). All these cadherins differ possess characteristic amino acid motifs in their first extracellular domain. Other subgroups of cadherins are the type II classic cadherins (named by numerals like, cadherin-6, -7, -8, and –10), protocadherins, desmosomal cadherins, Fat-like cadherins (Fat, Dachsous), cadherin-related molecules (e.g., Ret) and flamingo cadherins (CELSR cadherins). In my work, I mapped the expression of R-cadherin, cadherin-8 and cadherin-11.

The family of protocadherins contains a group of molecules that have 6 or 7 consecutive extracellular cadherin domains and show no homology to classic cadherins in their cytoplasmic domain. One of the cadherins investigated in my work, OL-protocadherin = protocadherin-10, is a member of the δ-protocadherin subfamily of protocadherins (Redies et al. 2005). Protocadherin subfamilies differ in the composition of their cytoplasmic domain and are found only in vertebrates where expression is especially prominent in the nervous system.

1.5.2 Cadherin expression in the cerebellar cortex

The expression of cadherins was first mapped in the cerebellar systems of chicken and mouse. The following conclusions were reached in these studies.

First, cadherins are expressed in distinct types of neurons during the development of the cerebellum (Fushimi et al., 1997; Arndt et al., 1998). The pattern of expression differs depending on the developing stage and, at least in some instances, it reflects the migratatory state of cerebellar neurons.

Second, several of the neuronal elements of the deep cerebellar nuclei and cerebellar-associated nuclei outside the cerebellum are marked by their expression of specific cadherins. For example, cadherins are expressed in regions of cerebellar cortex, which in turn project to parts of the deep cerebellar nuclei and to several nuclei in the hindbrain (Arndt and Redies, 1996; Fushimi et al., 1997; Korematsu and Redies, 1997a, 1997b; Suzuki et al., 1997; Arndt et al., 1998).

The afferent and efferent connections in the cerebellum are organized into parasagittal compartments. This organization pattern is reflected in the expression of several biochemical and molecular markers (reviewed in Hawkes and Mascher, 1994; Herrup and Kuemerle, 1997; Voogd and Glickstein, 1998). Cadherin-expression domains correspond to a subset of parasagittal domains of Purkinje cells, as first shown for R-cadherin in the chicken cerebellum by immunohistochemistry (Arndt and Redies 1996). Subsequently, similar parasagittal stripes of cadherin expression were found for cadherin-10 (Fushimi et al., 1997), cadherin-6B and cadherin-7 in the chicken (Arndt et al., 1998; Arndt and Redies, 1998), and for cadherin-8 (Korematsu and Redies, 1997a; Suzuki et al., 1997; Korematsu et al., 1997b) cadherin-6, cadherin-11 (Suzuki et al., 1997), and OL-cadherin (Hirano et al., 1999b) in the mouse. Recently, it has been shown that the classic cadherins function as a guide for migrating Purkinje cells in the cerebellum (Luo et al., 2004).

It has been shown in the chicken (Arndt et al., 1998), that the Purkinje cell clusters, which are expressing different cadherins, are separated by thin granule cell raphes (also called ribbons), as first described by Feierabend (1983). Other authors confirmed this general segmentation pattern in the chicken cerebellum by mapping the expression of other molecular markers (Lin and Cepko, 1998).

In this work, I will ask whether the raphe/ribbons are also observed during the development of the mouse cerebellum. My results show that cadherin-expressing, parasagittal Purkinje cell clusters are bordered by migrating granule cells also in the mouse. Thus, the raphe/Purkinje cell pattern is conserved between chicken and mouse.

1.5.3 Zebrins

There are many other antigens whose expression pattern reflects the parasagittal organization of Purkinje cell clusters in the cerebellum. Amongst these, the zebrins are probably the best-known examples. Two antigens are known: zebrin I (Hawkes et al., 1985; Hawkes and Leclerc, 1987), a 120-kD polypeptide, and zebrin II, a 36-kD polypeptide, which is a glycolytic isoenzyme aldolase c (Hawkes 1992). Zebrin I and II are Purkinje cell specific in the adult cerebellum and show nearly identical pattern of expression.

The zebrin-positive Purkinje cell clusters extend in a parasagittal, rostro-caudal direction throughout the vermis and the hemispheres and are separated by zebrin-negative Purkinje cell clusters. The positive bands are named P^+ and the negative bands P^-. The $P1^+$ band is running in the midline. Laterally, there are seven further P^+ bands on each side. An example is shown in Figures 4 and 8D.

Several biochemical and molecular markers share a similar pattern of expression as the zebrins. Briefly they are in rats: 5`-nucleotidase (Eisenman and Hawkes, 1990), cytochrome oxidase (Leclerc et al., 1990) and acetylcholinesterase (Boegman et al., 1988). In this work, I will show that OL-protocadherin relates also to the zebrin-positive compartments.

Genes expressed during cerebellar development are divided in two classes, the “early-onset” genes and the “late-onset” genes. This differentiation can be made on the basis of the expression patterns of several markers of parasagittal cerebellar organization. In my work, I will map the expression of zebrin II as an example of the “late-onset” genes. OL-protocadherin is expressed both during early and late development and can be used to compare directly the pattern established by early-onset and late-onset genes.

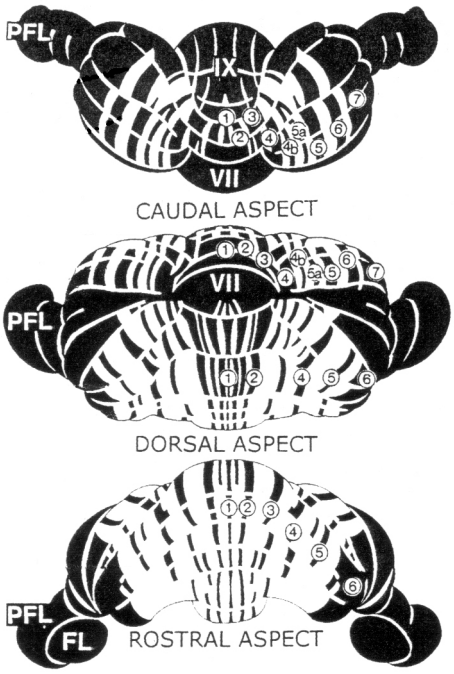

Fig. 4 The parasagittal banding pattern of zebrin II in the rat cerebellum. The zebrin II-positive Purkinje cell stripes are numbered. The medial zebrin II-positive Purkinje cell stripe is a single, numbered with "1". The following zebrin II-positive Purkinje cell clusters are numbered in mediolateral order. Some cerebellar lobules are marked by roman letters. The numbering is according to Hawkes and Leclerc. (*PFL*, paraflocculus; *FL*: flocculus). Taken and modified from Voogd and Glickstein (1998).

1.6 Cadherins in medicine

First described by Takeichi (1988), the cadherins have become a large and important family of cell adhesion molecules (CAMs) family. The cadherins can be found in different kinds of tissues in several organisms. Many biological studies show the important role of the cadherins in tissue organization and morphogenesis, not only in the neural system but in the entire organism.

In recent years, several reports have described the involvement of cadherins in the pathogenesis of diseases. Well investigated is the role of desmogleins, a relatively young subfamily of desmosomal cadherins, as the cause of pemphigus, a skin disease (Amagai et al., 1991). In this disease, the organism produces autoantibody against desmoglein, which is expressed at the surface of keratinocytes. Subsequently, there is loss of cell-cell adhesion, called acantolysis, between the keratinocytes which leads to the development of skin blisters.

A altered expression of the epithelial cadherin (E-cadherin) play a role in the developing of several tumors and their metastases, e.g. in melanocytic neoplasm (Cowley et al., 1996; reviewed by Smith et al., 2002), astrocytic tumors (Asano et al., 1997), neck,

lung, breast, thyroid, oesophageal, gastric, pancreatic, colon, hepatocellular, bladder, prostate, endometrial and ovarial carcinoma (reviewed by Winjnhoven et al., 2000).

Another function of cadherins and other cell adhesion molecules is the involvement in hormone-secreting processes. N-cadherin plays a role in the regulatory pathway of human growth hormone secretion (Rubinek et al., 2003).

These examples show, in brief, the role of cadherins in the pathogenesis of several diseases.

2. MATERIALS AND METHODS

2.1 Chemicals and instruments

2.1.1 Chemicals

• Acetic acid	Roth, Karlsruhe
• Acetic anhydride	Merck, Darmstadt
• Acetone	Merck, Darmstadt
• Anti-Digoxigenin-AP Fab fragments	Roche, Mannheim
• BCIP	Sigma-Aldrich, Deisenhofen
• Calcium chloride	Merck, Darmstadt
• Denhardt´s solution	Sigma-Aldrich, Deisenhofen
• Dextran sulfate	Sigma-Aldrich, Deisenhofen
• 3-3`Diaminobenzidintetrahydrochlorid	Sigma, Darmstadt
• Diethyl pyrocarbonate	Sigma, Darmstadt
• EDTA	Merck, Darmstadt
• Entellan embedding medium	Merck, Darmstadt
• Ethanol	Roth, Karlsruhe
• Ethidium bromide	Sigma-Aldrich, Deisenhofen
• Formamide	Merck, Darmstadt
• Glucose	Merck, Darmstadt
• HEPES	Sigma-Aldrich, Deisenhofen
• Histomount	Shandon, Pittsburgh, PA, USA
• Hoechst 33258	Sigma-Aldrich, Deisenhofen
• Horse serum	Vector Laboratories, Burlingame, CA, USA
• Hydrochloric acid	Merck, Darmstadt
• Hydrogen peroxide 30 %	Merck, Darmstadt
• Isopropanol	Merck, Darmstadt

- Levamisole — Sigma-Aldrich, Deisenhofen
- Magnesium chloride — Sigma-Aldrich, Steinheim
- Methanol — Merck, Darmstadt
- NaH_2PO_4 — Merck, Darmstadt
- Na_2HPO_4 — Merck, Darmstadt
- NaOH — Merck, Darmstadt
- NBT — Roche, Mannheim
- Nickel chloride — Merck, Darmstadt
- P-Silan — Serva, Heidelberg
- Paraformaldehyde — Merck, Darmstadt
- Phenol red — Merck, Darmstadt
- Potassium chloride — Merck, Darmstadt
- Ribonuclease A — Sigma-Aldrich, Deisenhofen
- Salmon DNA — Invitrogen, Karlsruhe
- Sheep serum — Sigma-Aldrich, Deisenhofen
- Skimmed milk — Merck, Darmstadt
- Sodium azide — Merck, Darmstadt
- Sodium acetate — Sigma-Aldrich, Deisenhofen
- Sodium chloride — Merck, Darmstadt
- Sodium citrate — Sigma-Aldrich, Deisenhofen
- Sucrose — Merck, Darmstadt
- Thionine acetate — Sigma-Aldrich, Deisenhofen
- Tissue-Tec O.C.T. medium — Miles, Elkhart, IL, USA
- Triethanolamine — Merck, Darmstadt
- Tris — ICN Biomedicals, Aurora, Ohio, USA
- Triton X-100 — Merck, Darmstadt
- Vectastain ABC-Elitekit — Vector Laboratories, Burlingame, CA, USA
- Vectashield medium — Vector Laboratories, Burlingame, CA, USA
- Xylenes — Roth, Karlsruhe
- Yeast t-RNA — Invitrogen, Karlsruhe

2.1.2 Instruments

- Bioclav — (Schütt) KSG, Olching

- Binocular stereomicroscope — Stemi SV 6, Zeiss, Oberkochen
- Centrifuge — IKA, Staufen
- Filter for sterilization — Pall Medical, Portsmouth, UK
- Fluorescence microscope — Axioplan, Zeiss, Oberkochen
- McIlwain tissue chopper — Gomshall, Surrey, England
- Refrigerated microtome — Leica, Nußloch
- Seesaw — GFL 3010, Burgwedel
- Slide glasses — SuperFrost Plus, Menzel Glaeser, Braunschweig
- Thermal unit — Strech A, Alessandrini, I-S. Prospero, Italy
- Ultraphot microscope — Zeiss, Oberkochen

2.1.3 Computer hardware and software

- Adobe Photoshop 5.5 — Adobe, Mountain View, CA, USA
- Freehand — Macromedia, San Francisco, CA, USA
- Microsoft Word — Microsoft, Redmond, WA, USA
- Power Macintosh 8000/120 — Apple, Silicon Valley, CA, USA
- Scanner Sharp JX — Sharp, Japan

2.2 Solutions for immunohistochemistry and in situ hybridization (ISH)

2.2.1 ABC reagent

- 100 µl solution A (avidin)
- 100 µl solution B (biotin with horseradish peroxidase)
- 75 µl horse serum
- add TBS solution to 5 ml

2.2.2 Acetic anhydride solution

- 380 µl acetic anhydride
- 380 µl hydrochloric acid
- 2.26 g triethanolamine
- 150 ml DEPC water

2.2.3 Solution containing alkaline phosphatase-conjugated Fab fragments against digoxigenin

- 1.5 µl anti-digoxigenin-AP Fab fragments
- 6 µl 10 % sodium azide (stock solution)
- 30 µl sheep serum
- add PBS solution to 3 ml

2.2.4 Blocking solution for immunohistochemistry

- 150 µl horse serum
- 320 µl 10 % Triton-X 100 (10 % solution)
- 40 µl 10 % sodium acid (10 % solution)
- 9.85 ml TBS solution

2.2.5 Blocking solution for in situ hybridization

- 200 µl sheep serum
- 10 ml PBS solution

2.2.6 Substrate solution for the staining reaction (in situ hybridization)

- 35 µl BCIP
- 45 µl NBT
- add levamisole solution (see 2.2.17) to 10 ml

2.2.7 Blocking solution for double immunofluorescent labeling

- 2.5 g dried skim milk
- 1.6 ml 10 % Triton-X 100 (10 % solution)
- 200 µl 10 % sodium azide (10 % solution)
- add 1x TBS solution (see 2.2.13) to 50 ml

2.2.8 Solution for the diaminobenzidine (DAB) reaction

- 75 µl DAB 40 %
- 50 µl $NiCl_2$ 0.04 %
- add TBS solution to 10 ml
- add 1 µl 30 % H_2O_2 solution in H_2O

2.2.9 Diethylpyrocarbonate (DEPC) –treated water

- 1 ml DEPC
- 9 ml 96 % ethanol
- add distilled water to 1l

2.2.10 Ethidium bromide staining solution

- 0.5 µl ethidium bromide (1 % solution)
- add 1x TBS (see 2.2.13) to 5 ml

2.2.11 Formamide solution

- 150 ml 100% formamide (stock solution)
- 150 ml 2x SSC solution

2.2.12 HEPES-buffered salt solution (HBSS, 10x stock solution)

- 1.4 M NaCl
- 50 mM KCl
- 50 mM glucose
- 4 mM Na_2HPO_4 x 2 H_2O
- 0.4 mM Phenol red
- 0.1 M HEPES
- add distilled water to 1 l
- pH 7.4

2.2.13 HBSS solution (1x)

- 100 ml HBSS stock solution (10x)
- 10 ml 1 M $MgCl_2$ (stock solution)
- 10 ml 1 M $CaCl_2$ (stock solution)
- add distilled water to 1 l

2.2.14 Hoechst staining solution

- 50 µg Hoechst 33258
- 100 ml TBS

2.2.15 Hybridizating solution A

- 1.5 ml formamide

- 60 µl 500mM EDTA
- 450 µl 20x SSC
- 60 µl 50x Denhardt`s solution
- 600 µl 50% dextran sulfate
- 330 µl DEPC water

2.2.16 Hybridizating solution B

- 5 µl yeast t-RNA
- 5 µl salmon DNA
- add cRNA probe, amount depending on its concentration
- 300 µl hybridizating solution A

2.2.17 Levamisole solution

- 50 mg levamisole
- 200 ml Buffer 3

2.2.18 NTE buffer

- 58.4 g NaCl
- 2.42 g Tris
- 0.74 g EDTA
- add DEPC water to 1l
- pH 8.0

2.2.19 PBS stock solution (10x, 1000 ml)

- 75.95 g NaCl
- 9.94 g Na_2HPO_4
- 3.6 g NaH_2PO_4
- add distilled or DEPC (for ISH) water to 1 l
- pH 7.4

2.2.20 4 % PFA in HEPES buffered solution (1000ml)

- 40 g paraformaldehyde
- 0.5 ml 1N NaOH solution
- 100 ml HBSS stock solution (10x)
- 10 ml 100 mM stock $CaCl_2$

- 10 ml 100 mM stock $MgCl_2$
- add 880 ml distilled water (60°C)
- pH 7.4

2.2.21 4 % PFA in PBS for ISH

- 20 g paraformaldehyde
- 500 ml 1x PBS

2.2.22 Proteinase-K buffer

- 12.1 g Tris
- 18.6 g EDTA
- add DEPC water to 1l
- pH 8.0

2.2.23 Proteinase-K solution

- 150 µl Proteinase-K stock solution (1 µg/ml)
- 150 ml Proteinase-K buffer

2.2.24 Ribonuclease A solution

- 300 µl Ribonuclease A (10 mg/ml stock solution diluted in NTE buffer)
- 150 ml NTE buffer

2.2.25 20x SSC solution

- 175.3 g NaCl
- 88.2 g sodium citrate
- add DEPC water to 1l
- pH 7.0

2.2.26 Sucrose solutions

- 12 % (w/v) sucrose 12 g sucrose in 100 ml HBSS solution (1x)
- 15 % (w/v) sucrose 15 g sucrose in 100 ml HBSS solution (1x)
- 18 % (w/v) sucrose 18 g sucrose in 100 ml HBSS solution (1x)

2.2.27 TBS stock solution (10x)

- 1.5 M NaCl

- 0.5 M Tris
- 35 ml hydrochloric acid
- add distilled water to 1 l
- 1 mM $CaCl_2$
- pH 7.4

2.2.28 TBS solution (1x)

- 1 l TBS stock solution (10x)
- add distilled water to 10 l

2.2.29 Thionine solution for Nissl staining

- 1 g thionine
- 100 ml 99 % ethanol
- 2.7 g sodium acetate
- 4.8 ml acetic acide
- add distilled water to 1 l

2.2.30 Tris buffer 3

- 12.1 g Tris
- 5.84 g NaCl
- 10.1 g $MgCl_2$
- add distilled water to 1l
- pH 9.5

2.2.31 Tris buffer 4

- 1.21 g Tris
- 0.37 g EDTA
- add distilled water to 1l
- pH 8.0

2.2.32 Preparation of the slide glasses for in situ hybridization

- continuous washing of the slide glasses with water for 2 hours
- 2x short washing with distilled water
- 6 hours or overnight baking of the slide glasses at 180 °C
- 10 – 30 seconds in 2 % P-silane solution in acetone

- 2x 10 minutes washing in acetone
- 10 minutes washing in DEPC water
- dry at room temperature

2.2.33 Solution for the wet chamber

- 10 ml formamide
- 2 ml 20x SSC
- 8 ml DEPC water

2.3 Antibodies for immunohistochemistry

2.3.1 Primary antibodies

Calbindin, monoclonal mouse antibody against chicken calbindin-D (clone CL-300; Sigma, Deisenhofen, Germany)
1:1000 dilution

5G10, monoclonal rat antibody against a GST fusion protein of the cytoplasmic domain of an isoform of OL-protocadherin (kind gift of Dr. S. Hirano, RIKEN for Developmental Biology, Kobe, Japan; Aoki et al., 2003)
1:200 dilution

4D7/TAG-1, monoclonal mouse antibody against rat TAG-1, developed by M. Yamamoto, obtained from the Developmental Studies Hybridoma Bank maintained by the University of Iowa, Department of Biological Sciences, Iowa City, IA 52242, under contract NO1-HD-7-3263 from the NICHD (Dodd et al. 1998)
1:50 dilution

Zebrin II, monoclonal mouse antibody against aldolase C (kind gift of R. Hawkes, University of Calgary; Brochu et al. 1990; Ahn et al. 1994)
1:200 dilution

2.3.2 Secondary antibodies

Cy3 (indocarbocyanine dye) -conjugated polyclonal goat antibody against mouse IgG
Dianova, Hamburg
1:400 dilution

Polyclonal biotinylated goat antibody against rat IgG
Dianova, Hamburg
1:1000 dilution

Polyclonal biotinylated horse antibody against mouse IgG
Vector Laboratories, Burlingame, CA, USA
1:200 dilution for calbindin
1:1000 dilution for Zebrin II
Polyclonal biotinylated goat antibody against mouse IgM
Dianova, Hamburg
1:500 dilution

2.4 cRNA probes and antibodies for in situ hybridization

2.4.1 Digoxigenin-labeled antisense cRNA probes for in situ hybridization

Digoxigenin-labeled probes were kindly transcribed in vitro by Ulrike Laub from the following plasmids with appropriate polymerases (T3, T7 or SP):

mcad8-12, containing a 1.6-kb fragment of mouse cadherin-8 cDNA from the 5´region (Korematsu and Redies 1997b)

pSP73, containing the 2.5-kb *Sma*I-*Pst*I fragment of mouse cadherin-11 cDNA (kind gift of Drs. Y. Kimura and M. Takeichi, Kyoto University; Kimura et al. 1995)

pBSMR4, containing full-length mouse R-cadherin cDNA (kind gift of Drs. H. Matsunami and M. Takeichi; Matsunami and Takeichi 1995)

Mpr-655, containing the *Hind*III-*Xba*I fragment of mouse TAG-1 cDNA (kind gift of Dr. S. Kozlov, University of Zürich; Wolfer et al. 1998)

2.4.2 Antibodies for in situ hybridization

Alkaline phosphatase-conjugated Fab fragments against digoxigenin (Boehringer, Mannheim, Germany)

2.5 Animals

Pups from C57BL mice were deeply anesthetized on ice and decapitated. Staged pregnant C57BL mice were deeply anesthetized by inhalation of diethyl ether and killed by cervical dislocation. These procedures were in accordance with the current version of the German Law on the Protection of Animals and institutional guidelines on the use of animals in research. Brains were dissected and fixed in 4% formaldehyde dissolved in HEPES-buffered salt solution supplemented by 1 mM Ca^{2+} and 1 mM Mg^{2+} (HBSS, see: *2.2.13*) for 2 hours. Following cryoprotection in 12%, 15% and 18% sucrose in HBSS (see: *2.2.26*) for 2 hours each, brains were mounted in Tissue-Tek O.C.T. compound, frozen in liquid nitrogen and stored at –80°C. The following stages were used: embryonic day 16 (E16), E18, postnatal day 0 (P0), P2, P3, P4, P5, P7, P10 and P14. The day of birth was designated as P0. All animals were obtained from the animal facilities at the University of Essen School of Medicine.

2.6 Immunhistochemistry

Cerebella of P2, P3, P5, P7, P10, P14 and P21 mouse pups were prepared in HBSS under a binocular stereomicroscope. The tissue was treated as described in Section 2.5. Cerebella were cut into transverse series of 20µm thick slices in a refrigerated microtome and dried at 37°C on coated slide glasses. The sections were postfixed in 4 % formaldehyde/HBSS (see: 2.2.20) on ice for 15 minutes and washed in distilled water and then in Tris-buffered saline (TBS, see: 2.2.28) for 15 minutes. To permeabilize cell membranes and inactivate endogenous peroxydase, the sections were treated in –20°C methanol containing 0.3 % H_2O_2 for 30 minutes. After this, the slices were washed in TBS supplemented by 3-5 ml Triton X100 (10 % solution) to reduce surface tension (TBS/Triton X100) for 15 minutes at room temperature. The same blocking solution as for double immunofluorescent labeling (see: 2.2.7) was used for immunohistochemistry to block non-specific binding and to dilute the antibodies. Only for immunostaining with the calbindin-antibody, a horse serum containing blocking solution was used. In both cases, the cerebellar tissue was incubated with blocking solution for 30 minutes at room temperature.

The primary antibodies used are listed above (see: 2.3.1). The sections were incubated with the primary antibodies, which were diluted with the horse serum-blocking solution, overnight at 4°C.

On the second day of immunostaining, the slices were washed for about 10 minutes with TBS, followed by TBS/Triton X-100 for 5 minutes. For detection of primary antibodies, appropriate secondary antibody labeled with biotin was incubated for about 1

hour. The sections were washed again in TBS and TBS/Triton X-100 for 20 and 10 minutes, respectively. The biotin-labeled antibodies were detected using a commercially available kit (Vector ABC Elite kit, Vector Laboratories, see: 2.2.1) containing avidin (solution A), biotin with horseradish peroxidase (solution B) and 1.5 % horse serum. Reagents were diluted in TBS and sections incubated for about 30 minutes. Afterwards, the slices were washed again with TBS and TBS/Triton X-100, as described above, for 30 minutes. The enzymatic staining reaction with 0.7 % diaminobenzidine and 0.5 % $NiCl_2$ diluted in TBS (see: 2.2.8) was started by adding 0.01 % H_2O_2 and stopped by washing with TBS, after enough reaction product had formed.

Sections not used for double staining with a nuclear dye were dehydrated in an ascending series of ethanol (70 %, 96 %, 100 %) for 10 minutes each, once in isopropanol for 10 minutes, and two times in xylenes for 20 minutes. The slices were then embedded in Histomount.

To visualize cell nuclei, some immunostaind slices were washed in TBS and counter-stained with 0.0001 % ethidium bromide for 10 minutes in a dark chamber. These sections were mounted with Vectashield medium (Vector Laboratories, Burlingame, CA, U.S.A.).

All sections were viewed and photographed under a light transmission microscope equipped for epifluorescence detection (Axioplan, Zeiss, Oberkochen). Processing of scanned images was carried out on a computer using the Photoshop program (Adobe, Mountain View, CA).

2.7 Schematic reconstruction of raphes by calbindin immunoreactivity in P5 cerebellum

For a reconstruction of calbindin immunoreactivity in P5 cerebellum, a complete series of calbindin-immunostaind sections was obtained and counterstained with a nuclear dye (ethidium bromide). These sections were spaced 40 µm apart. Subsequently, the sections were immunostaind, dehydrated in ethanol and mounted as described in Section 2.6. Immunostaining of all sections was photographed with a digital camera. The position of all gaps of immunoreactivity in the prospective Purkinje cell layer and/or of nuclear ribbons in the molecular layer (see Results section) was detected through the microscope at high magnification and marked on digitized sections. After the identification of the lobules, the position of the gaps was transferred onto anterior and posterior angled schematic views of P5 cerebellum (modified after color Figures 4B and 5B in Altman and Bayer, 1997).

2.8 Double immunofluorescent labeling

Cerebella of P3 and P5 mouse pups were isolated in HBSS under a binocular stereomicroscope. The tissue was treated as described in Section 2.5. The brain was cut in a transverse plane in a refrigerated microtome into sections of 20 µm thickness and dried on coated slide glasses for 30 minutes. The slices were postfixed in 4 % formaldehyde/HBSS (see 2.2.20) on ice for 15 minutes and then washed in Tris-buffered saline (TBS, see 2.2.28) containing 1mM $CaCl_2$ for 15 minutes at room temperature.

The nonspecific binding in the tissue was reduced by a blocking solution containing TBS, 5 % dried skim milk, 0.3 % Triton and 0.04 % sodium azide (see 2.2.7). The sections were incubated for 30 minutes in the blocking solution.

As primary antibody, mouse monoclonal antibody against chicken calbindin-D (clone CL-300; Sigma, Deisenhofen, Germany) was used. The sections were incubated with the primary antibodies, which were diluted 1:1000 with the blocking solution, overnight at 4 °C.

On the second day, the slices were washed for about 10 minutes with TBS and with TBS/Triton X-100 for 5 minutes. For detection of the primary antibody, appropriate antibody labeled with the indocarbocyanine dye Cy3 (polyclonal goat antibody against mouse IgG) was used. The tissue was incubated for 30 minutes at room temperature. The antibody was diluted in the skimmed milk blocking solution. The sections were washed again in TBS for about 10 minutes and in TBS/Triton X-100 for 5 minutes. After washing in TBS, the sections were incubated in a dark chamber for 10 minutes at 4°C with nuclear dye, Hoechst 33258 (see 2.2.14). Then the slices were washed once more in TBS for 15 minutes and embedded in Vectashield medium. All sections were viewed and photographed under a light-transmission microscope equipped for epifluorescence detection (Axioplan, Zeiss, Oberkochen). Processing of scanned images was carried out on a computer using the Photoshop program (Adobe, Mountain View, CA).

2.9 In situ hybridization

Cerebella of E11, P0, P2, P3 and P4 mouse pups were isolated in HBSS under a binocular stereomicroscope. The tissue was treated as described in Section 2.5. Transversal series of the mounted cerebella were cut into 20µm thick slices in a refrigerated microtome and dried at 37 °C on silane-coated slide glasses (see *2.2.32*). The sections were postfixed in 4 % formaldehyde/HBSS (see *2.2.20*) on ice for 30 minutes and washed in phosphate-buffered saline (PBS, see *2.2.19*) for 10 minutes. For better penetration of the anti-sense probe into the cells, the tissue was permeabilize by treatment with proteinase K solution (1

µg/ml), washed again in PBS for 5 minutes and postfixed in 4% formaldehyde/HBSS for 30 minutes. After washing in PBS for five minutes the slices were incubated with acetic anhydride solution (see *2.2.2*) for 10 minutes to hydrolyze the cellular mRNA or DNA partly in order to prevent unspecific binding of the anti-sense probe. Again the slices were washed in PBS solution for 10 minutes.

For hybridization the following digoxigenin-labeled anti-sense cRNA probes were used: mcad8-12 containing a 1.6 kb fragment of mouse cadherin-8 cDNA from the 5' region (Korematsu and Redies 1997b); pSP73 containing the 2.5 kb SmaI-PstI fragment of mouse cadherin-11 cDNA (kind gift of Drs. Y. Kimura and M. Takeichi, Kyoto University); pBSMR4 containing full-length mouse R-cadherin cDNA (kind gift of Drs. H. Matsunami and M. Takeichi); and Mpr-655 containing the HindIII-XbaI fragment of mouse TAG-1 cDNA (kind gift of Dr. S. Kozlov, University of Zurich).

The anti-sense probes were diluted in hybridization solution B (see: *2.2.16*) including yeast mRNA and salmon DNA to minimize the background staining and the hybridization solution A (see *2.2.16*) including formamide and SSC, to increase the binding of the cRNA probe to the specific binding domains and to decrease the hybridization temperature, respectively.

After overnight hybridization with the cRNA probes in a wet chamber, sections were washed in 5x SSC solution, formamide solution (see: *2.2.11*), Tris buffer (NTE-buffer, see *2.2.18)* and treated with ribonuclease A (20 µg/ml in NTE buffer, see: *2.2.24*) for 30 minutes to eliminate the unspecifically bound cRNA probes. Again the slices were washed in NTE buffer, formamide solution, 2x SSC and 0.1x SSC for 20 minutes each and in PBS for at least 10 minutes.

Digoxigenin-labeled cRNA were detected with alkaline phosphatase-conjugated Fab fragments against digoxigenin (Boehringer, Mannheim, Germany). The unspecific antibody binding domains were blocked by incubating the tissue with 2% sheep serum (see: *2.2.5*) for about 40 minutes. To visualize alkaline phosphatase bound in the tissue, a coloring reaction with X-phosphatase and nitroblue tetrazolium salt as substrate was carried out. Sections were either dehydrated and mounted in Entellan (Merck, Darmstadt, Germany) or counterstained for nuclei with ethidium bromide (1 µg/ml in TRIS-buffered saline) and mounted in Vectashield medium.

All sections were viewed and photographed under a light-transmission microscope equipped for epifluorescence detection (Axioplan, Zeiss, Oberkochen). Processing of scanned images was carried out on a computer using the Photoshop program (Adobe, Mountain View, CA).

2.10 Nissl staining

Sections adjacent to those used for immunohistochemistry were stained to visualize Nissl substance in neurons. Dried sections were washed in distilled water and then dehydrated in 70% ethanol for 10 minutes. After a brief wash in distilled water, the sections were incubated in thionine solution (see *2.2.29*) for 5 minutes. The sections were then washed in distilled water for 2 minutes and differentiated in an ascending ethanol series (70 %, 96 %, 100 % in distilled water). Next, the slices were incubated for 10 minutes in isopropanol and washed twice in xylenes. The slices were embedded in Histomount and photographed under a transmission light microscope (Ultraphot, Zeiss, Oberkochen, and Axiophot, Zeiss, Oberkochen).

3. RESULTS

Figure 5 shows a complete transverse section through the postnatal day 4 (P4) mouse cerebellum hybridized in situ with antisense probe for cadherin-8 (Fig. 5A) and counterstained with a nuclear dye (Fig. 5B). A similar transverse section through P5 cerebellum immunostaind for OL-protocadherin is shown in Fig. 6A. As demonstrated previously (Korematsu and Redies, 1997a; Hirano et al. 1999), cadherin-8 and OL-protocadherin are each expressed by clusters of immature Purkinje cells (Fig. 5A, arrowheads in Fig. 6A). Note that the two cadherins show distinct expression patterns, as previously demonstrated on whole-mount specimens (Suzuki et al. 1997; Hirano et al. 1999). Cadherin-8-positive Purkinje cell clusters are found in all lobules, except lobules I-III. Purkinje cell clusters immunoreactive for OL-protocadherin are also found in all lobules, except lobule I.

In the chicken, granule cell raphes are frequently found at the borders of cadherin-expressing Purkinje cell clusters (Arndt et al. 1998). We therefore searched for granule cell raphes at the borders of cadherin-expressing Purkinje cell clusters also in the mouse. A nuclear stain of a section through lobules IV-VIII (Fig. 5B) reveals thin ribbons of cell nuclei at the majority of borders of the cadherin-8-positive Purkinje cell clusters (arrows in Fig. 5B).

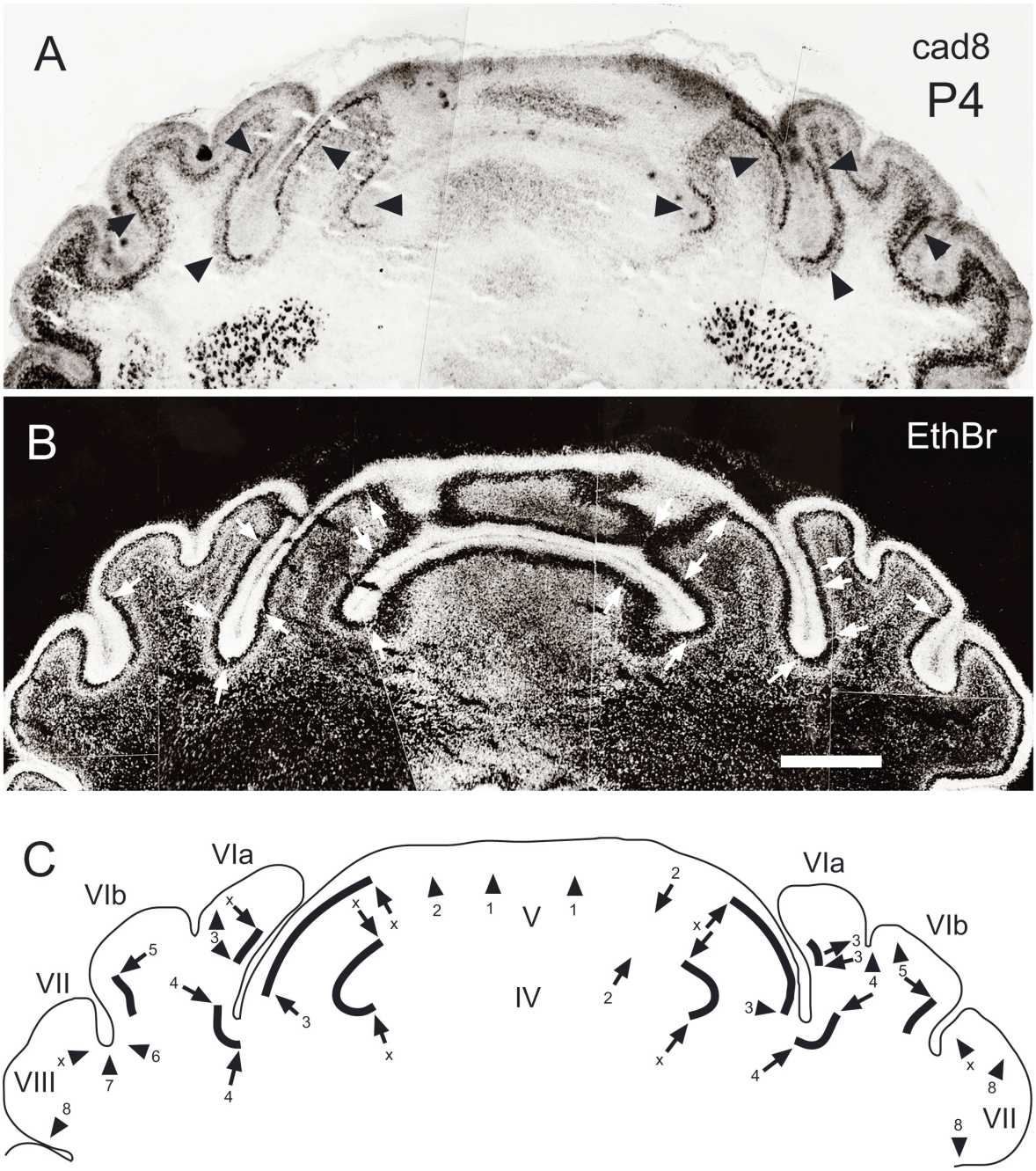

Fig. 5A-C Spatial relationship between cadherin-8-expressing Purkinje cell clusters and ribbons of cell nuclei ('raphes') in the molecular layer. A transverse section through a P4 mouse cerebellum was hybridized *in situ* with anti-sense probe for cadherin-8 (cad8, **A**) and counterstained for cell nuclei with ethidium bromide (*EthBr* in **B**). The schematic drawing in **C** shows the spatial relationship between the cadherin-8-positive Purkinje cell clusters (*arrowheads* in **A**, *thick lines* in **C**) and the nuclear ribbons (*arrows* in **B**, **C**). The *arrowheads* in **C** indicate the position of ribbons that were detected in immediately adjacent sections. *Arabic numerals* mark individual ribbons that extend over almost all lobules, as depicted in Fig. 10. The letter *x* indicates the position of additional ribbons. *Roman numerals* mark the cerebellar lobules. Bar 500 µm.

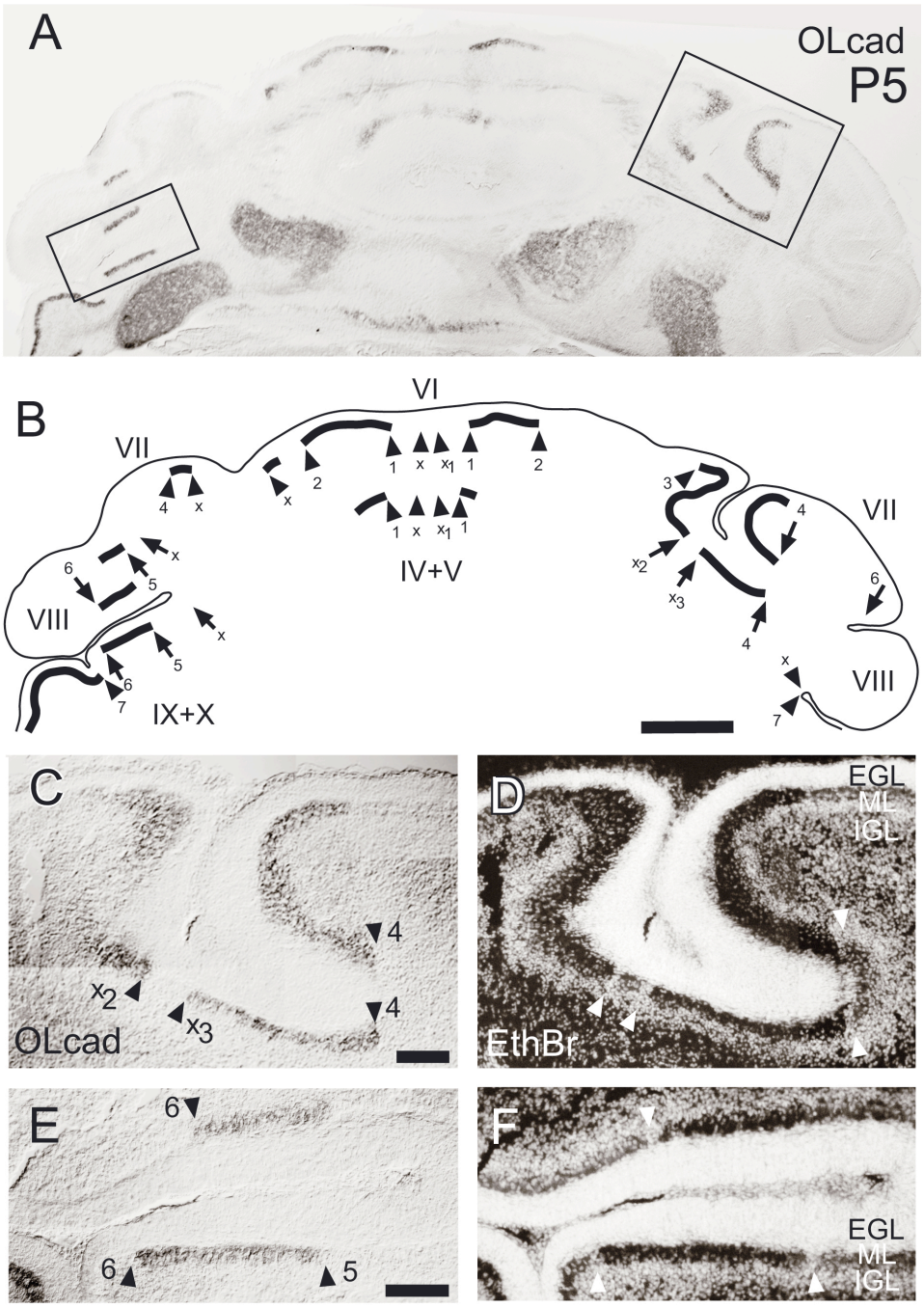

Fig. 6A-F Spatial relationship between OL-protocadherin-positive Purkinje cell clusters and ribbons of cell nuclei (raphes) in the molecular layer (*ML)*. A transverse section through a P5 mouse cerebellum was immunostaind with antibodies against OL-protocadherin (*OL-cad* in **A**) and counterstained with the nuclear dye ethidium bromide (*EthBr*, data not shown). The schematic drawing in **B** shows the spatial relationship between the OL-protocadherin-positive Purkinje cell clusters (*thick lines in **B***) and the nuclear ribbons detected on the same section (*arrows*) or on the immediately adjacent section (*arrowheads*). **C** and **E** show the areas *boxed* in **A** at a higher magnification and viewed with differential interference contrast, together with the corresponding nuclear stains (**D**, **F**). The *arrowheads* in **C**-**F** indicate the position of the ribbons (compare with **B**). *Arabic numerals* mark individual ribbons that extend over almost all lobules, as depicted in Fig. 6. The letter *x* indicates the position of additional ribbons. *Roman numerals* mark the cerebellar lobules. (*EGL* external granule layer, *IGL* internal granule layer). *Bars* **A**, **B** 400 µm; **C**-**F** 100 µm.

The ribbon pattern is symmetrical about the midline. Additional ribbons bordering the cadherin-8-positive cell clusters were identified on nuclear stains of immediately adjacent sections (arrowheads in Fig. 5C). Similar findings were obtained for the OL-protocadherin-positive Purkinje cell clusters (data not shown). Figures 5C and 6B show schematic superpositions of the cadherin-8-positive Purkinje cell clusters (thick lines) and the positions of all ribbons of the cadherin-positive Purkinje cell clusters (thick lines) and the positions of all ribbons of cell nuclei detected in the section shown (arrows in Figs. 5C, 6B) and in immediately adjacent sections (arrowheads in Figs. 5C, 6B), confirming the extensive spatial coincidence between the two types of structures in lobules IV-VIII (Fig. 5C) and lobules IV-X (Fig. 6B) respectively. The borders of cadherin-expressing Purkinje cell clusters in the other lobules show a similarly frequent coincidence with the ribbons. Note, however, that a few borders of the cadherin-positive Purkinje cell clusters do not coincide with ribbons of cell nuclei (3 out of the 20 borders shown for cadherin-8 in Fig. 5C, and 7 out of 26 borders shown for OL-protocadherin in Fig. 6B). Vice versa, many nuclear ribbons do not form the borders of cadherin-positive Purkinje cell clusters (17 out of the 33 ribbons shown in Fig. 5C, and 9 out of 28 ribbons shown in Fig. 6B). Similar results were obtained for the other lobules containing clusters of Purkinje cells expressing cadherin-8 or OL-protocadherin.

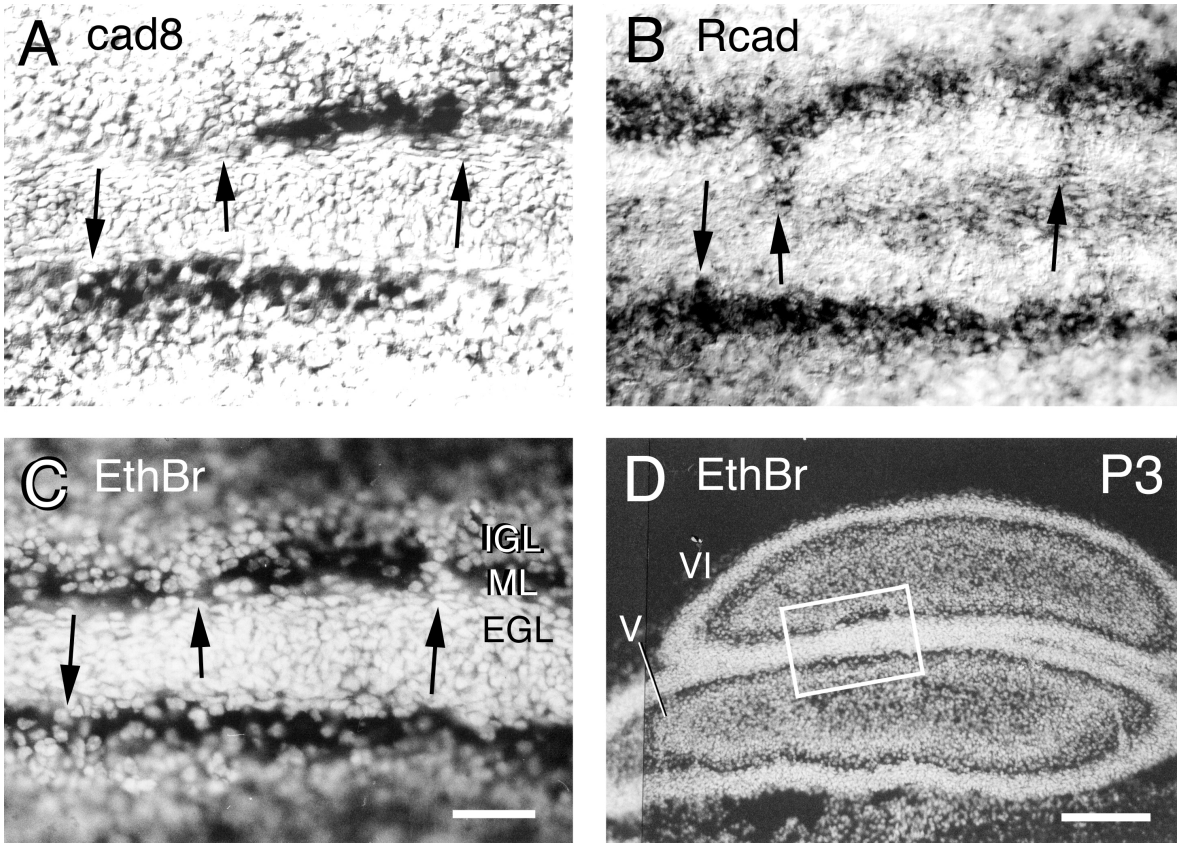

Fig. 7A-D Cadherin-8-expressing Purkinje cell clusters bordered by R-cadherin-expressing nuclear ribbons (raphes) in the molecular layer. Adjacent transverse sections through a P3 mouse cerebellum were hybridized *in situ* with anti-sense probes for cadherin-8 (*cad8*, **A**) and R-cadherin (*Rcad*, **B**). The section shown in **A** was counterstained for cell nuclei with ethidium bromide (*EthBr*; **C**, **D**). The *arrows* in **A-C** indicate the position of the nuclear ribbons. **A-C** show enlargements of the area boxed in **D**. *Roman numerals* mark the cerebellar lobules. (*IGL*, internal granular layer; *EGL*, external granular layer; *ML*, molecular layer). *Bars*, **A-C** 50 µm, **D** 200 µm.

Figure 7 shows, at a higher magnification, three nuclear ribbons (arrows in Fig. 7C) bordering two cadherin-8-positive Purkinje cell clusters (Fig. 7A) in lobules V and VI of P3 cerebellar cortex. For OL-protocadherin, similar findings are presented in Fig. 6C-F. The ribbons are characterized by a higher density of cell nuclei. Cell nuclei are also found dispersed throughout the developing molecular layer but at much lower density (Figs. 7C, 6D, 6F).

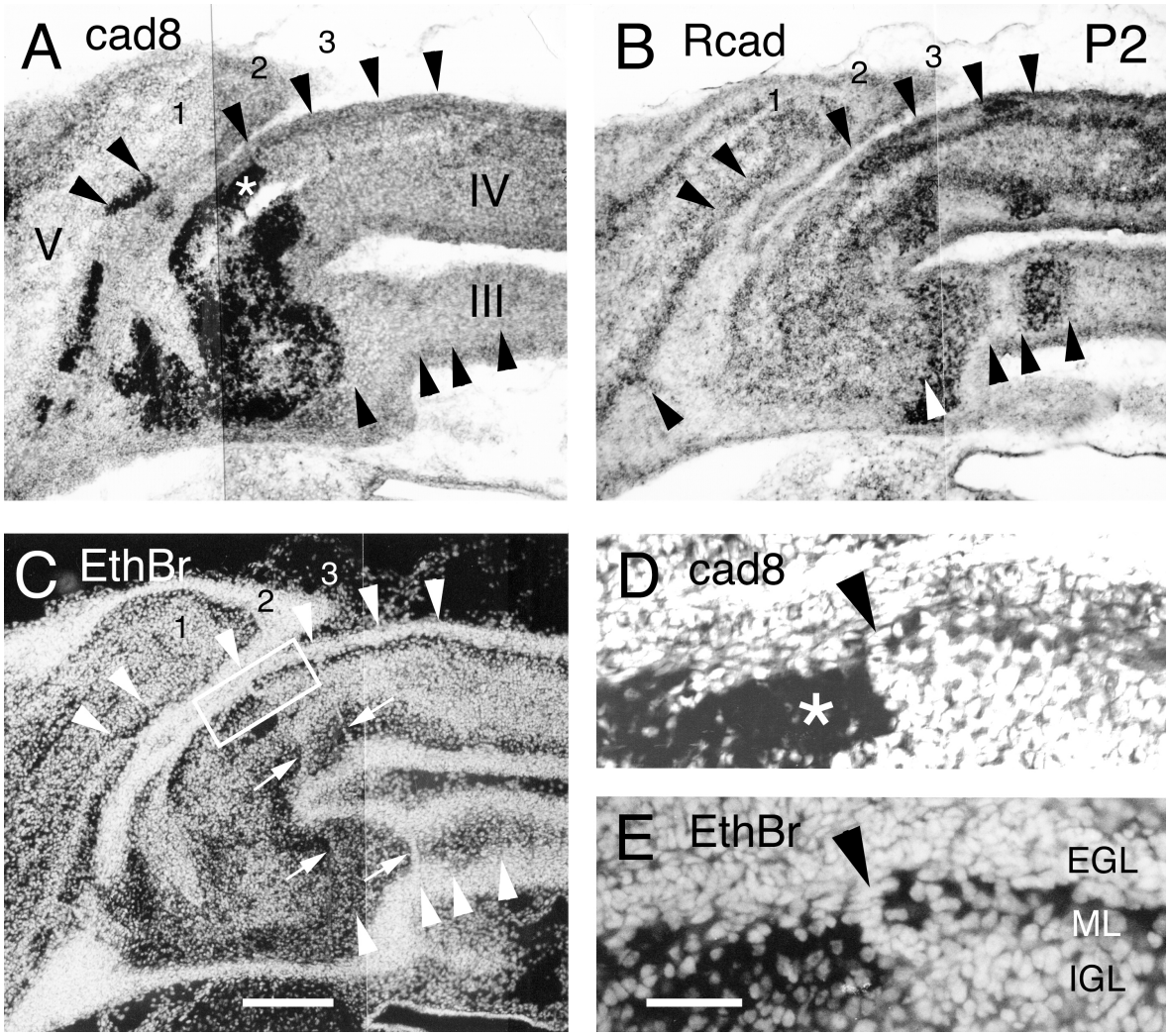

Fig. 8A-E Segments of cadherin-expressing Purkinje cells separated by nuclear ribbons (raphes) in the molecular layer. Transverse sections through P2 cerebellum were hybridized *in situ* with anti-sense probes for cadherin-8 (*cad8* in **A**) and R-cadherin (*Rcad* in **B**). The section shown in **A** was counterstained with ethidium bromide for cell nuclei (*EthBr* in **C**). *Arrowheads* mark the borders between the Purkinje cell segments differentially expressing cadherins; some of the segments are numbered (*1-3*). At some of the borders, nuclear ribbons are seen that extend parasagittal across two lobules (*arrows* in **C**). The cadherin-8-positive segment 1 (*asterisk* in **A** and **D**) is shown at a higher magnification in **D**, together with the corresponding nuclear stain (**E**). The *arrowheads* in **D** and **E** point to a nuclear ribbon in the molecular layer. *Roman numerals* mark the cerebellar lobules. (*EGL*, external granular layer; *IGL*, internal granular layer; *ML*, molecular layer). *Bars* in **A-C** 200 µm, in **D**, **E** 50 µm.

As in the chicken (Arndt and Redies 1996), some Purkinje cell clusters express R-cadherin. These clusters are partially complementary to the cadherin-8-positive clusters. For example, Figure 8 shows several segments of Purkinje cells (between arrowheads) that differentially express the two cadherins in lobules III-V of the P2 cerebellum. The segment marked '1' expresses cadherin-8 (Fig. 8A, D) but not R-cadherin (Fig. 8B) while the segment marked '2' expresses R-cadherin but not cadherin-8. Neither of the two cadherins

is expressed in the segment marked ‘3’. The segment marked ‘1’ is separated from that marked ‘2’ by a nuclear ribbon (Fig. 8E). With few exceptions, nuclear ribbons also border the other cadherin-expressing segments (arrows in Fig. 8C). The cadherin-expressing Purkinje cell segments and the intervening nuclear ribbons can be seen in lobules III, IV and V at corresponding positions. R-cadherin-positive cells are also found in the external and internal granular layers at P2 (Fig. 8B).

Compared with similar ribbons in the chicken (Arndt et al. 1998; see also Discussion), the ribbons in the mouse are less conspicuous, and it was sometimes difficult to clearly distinguish the ribbons from more loosely dispersed cell nuclei in the molecular layer. Complete series of sections through the entire cerebellar cortex at P3-P5 show nuclear ribbons in all cerebellar lobules. Frequently, the ribbons can be followed from section to section over several lobules, indicating that they extend parasagittal over large parts of the cerebellar cortex. Given their parasagittal extent, we attempted a complete reconstruction of the ribbon system in the cerebellar cortex of the postnatal mouse. For this purpose, the Purkinje cell segments were stained with an antibody against calbindin. As shown previously by Wassef et al. (1985), the Purkinje cells are compartmentalized and there are gaps of calbindin immunoreactivity at regular intervals in the prospective Purkinje cell layer. Double-labeling of a complete series of sections from P3 cerebellum with calbindin antibody and nuclear dye revealed that the gaps (Fig. 9B) are regularly found at a position directly beneath a nuclear ribbon (Fig. 9A). In our experience, the gaps are discernible somewhat more easily and can be followed more consistently from section to section than the ribbons. The positions of the ribbons and/or gaps were mapped over the entire cerebellar cortex in a complete series of sections through P5 cerebellum. The positions were transferred onto anterior and posterior views of the P5 cerebellum, as shown in the schematic diagram displayed in Figure 10. Results reveal that eight ribbons/gaps extend over almost all cerebellar lobules, and these were numbered in Fig. 6. Additional ribbons/gaps are found only in specific lobules (e.g., see lobules IV-VI in Fig. 10). Consequently, the lobules differ in the number of ribbons/gaps they contain. Generally, the lobules with a larger medio-lateral extent contain more ribbons/gaps. Most lobules contain 9-12 ribbons/gaps. Nearly, all of the eight ribbons/gaps that extend over the entire cerebellar cortex coincide with borders of Purkinje cell cluster that are positive for cadherin-8 or for OL-protocadherin (Figs. 5C, 6B)

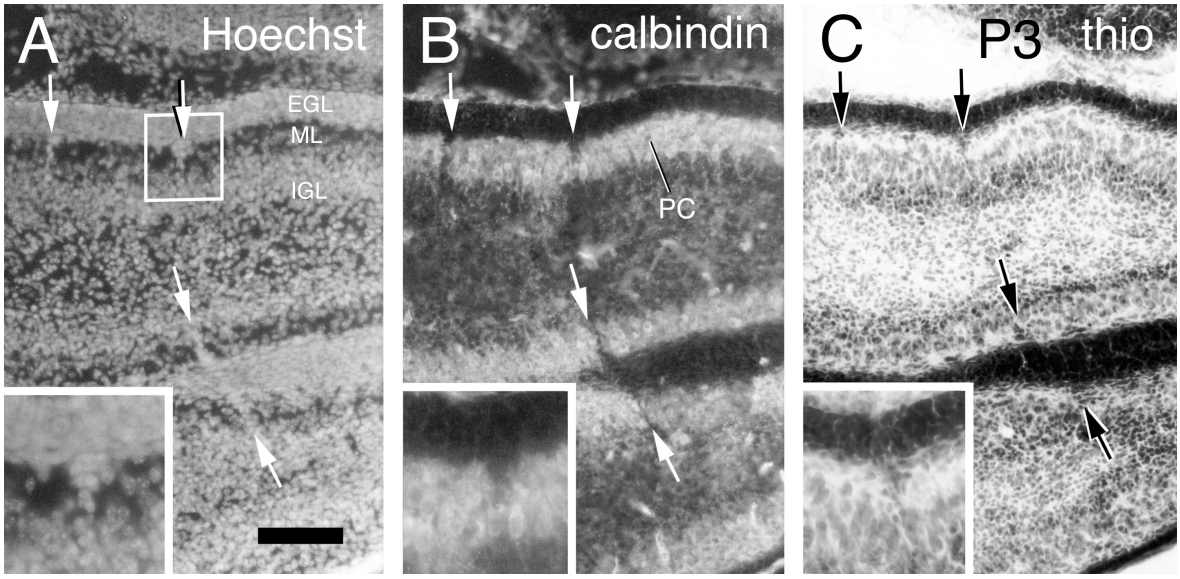

Fig. 9A-C Position of nuclear ribbons (raphes) in the molecular layer in relation to calbindin immunoreactivity and Nissl stains. A transverse section through P3 cerebellum was immunostaind with an antibody against calbindin (**B**) and counterstained with nuclear dye Hoechst 33258 (*Hoechst* in **A**). An adjacent section was stained for Nissl substance with thionine (*thio* in **C**). The *arrows* point to the positions of nuclear ribbons in the molecular layer; these positions coincide with gaps in the calbindin immunostain. The *inserts* in each panel show magnifications of the area boxed in **A**. *Roman numerals* mark the cerebellar lobules. (*IGL*, internal granular layer; *EGL*, external granular layer; *ML*, molecular layer; *PC*, Purkinje cells). *Bar* 100 µm.

Appearance and molecular characteristics of nuclear ribbons in development

At E16 and E18, the molecular layer is relatively thin and no ribbons of increased cell density could be observed. On nuclear stains, ribbons in the molecular layer are first seen at around P0. At this stage of development, R-cadherin is expressed by dispersed cells in the nuclear ribbons (arrowheads in Fig. 11B) and in other parts of the molecular layer (arrows in Fig. 11B). Most (if not all) cells in the external and internal granular layers express cadherin-11 (Fig. 11C). Some of the nuclear ribbons are also cadherin-11 positive (arrowheads in Fig. 11C). At P3, most of the cells in the nuclear ribbons express R-cadherin (Fig. 11B). R-cadherin is also strongly expressed in the internal granular layer. In the external granular layer, only weak expression is seen at P3. The ribbons of cells can even be seen on Nissl stains (Fig. 9C). The staining and density of the ribbon cells is similar to the cells of the innermost sheet of the external granular layer (insert in Fig. 9C). We did not observe any TAG-1 expression (Furley et al. 1990; Stottmann and Rivas 1998) in the nuclear ribbons by *in situ* hybridization or immunostaining.

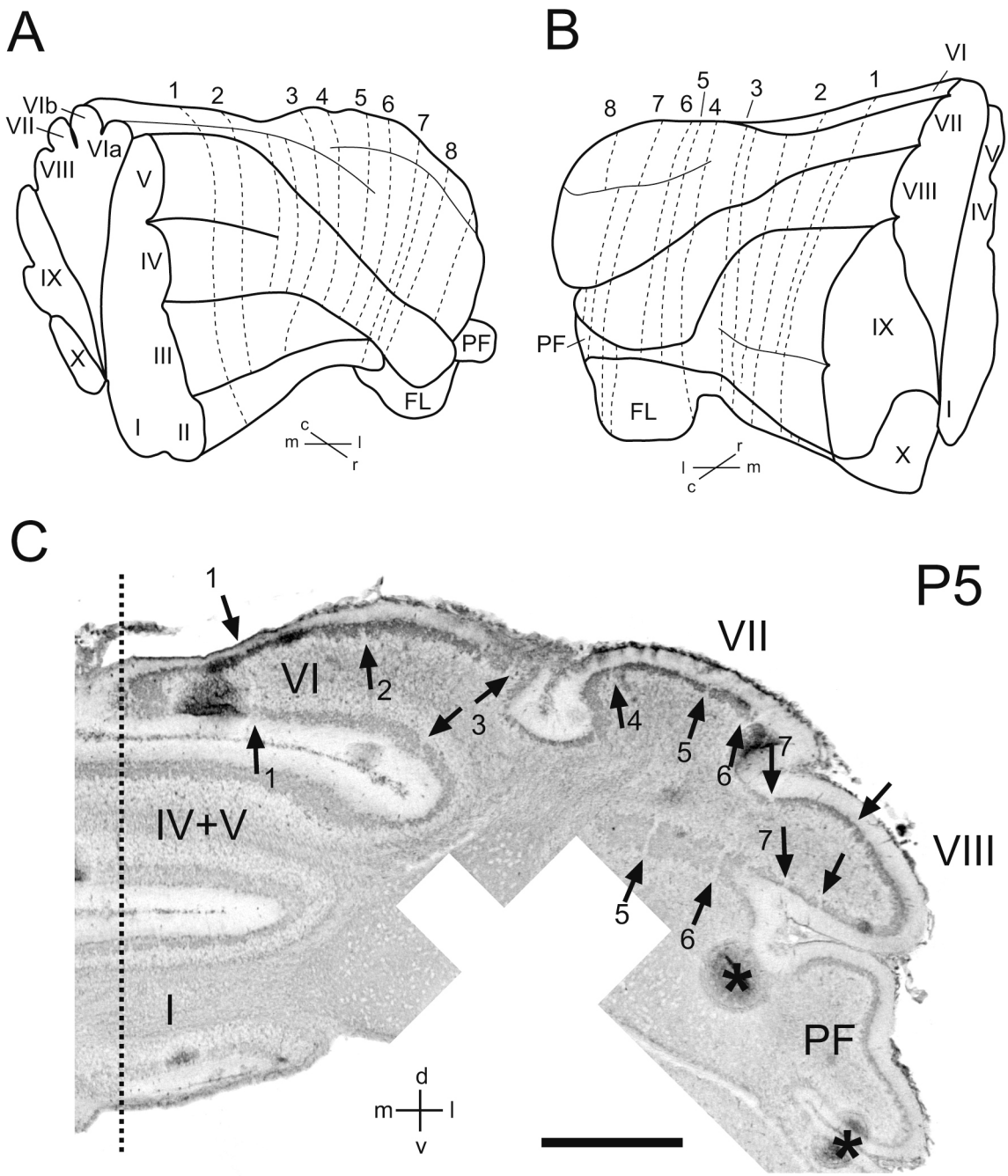

Fig. 10A-C Complete schematic reconstruction of raphes in the P5 cerebellum shown from an anterior angled view (**A**) and a posterior angled view (**B**; cerebellar outlines modified after color figures 8B and 9B, respectively, by Altman and Bayer, 1997). The analysis was based on a series of transverse sections doubly stained with calbindin antibody and nuclear dye. One representative calbindin-stained section from this series is shown in **C**. The *dashed lines* in **A** and **B** represent the position of the raphes. *Arabic numerals* mark individual raphes which extend from anterior (**A**) to posterior lobules (**B**). *Roman numerals* mark the cerebellar lobules. The *arrows* in **C** point to raphes, as indicated by the gaps in the calbindin staining and/or nuclear ribbons. *Arabic numerals* in **C** refer to individual raphes, as indicated in **A** and **B**. *Asterisks* in **C** mark artifacts. The *dashed line* in **C** represents the midline (*c* caudal; *d* dorsal; *FL* lobulus flocculo-nodularis; *m* medial; *l* lateral; *PF* paraflocculus; *r* rostral; *v* ventral). *Bar* **C** 500 µm.

However, the TAG-1-positive external granular layer occasionally formed a shallow bulge into the molecular layer at the position of some of the nuclear ribbons (data not shown). Ribbons are still seen at P6 but, from P7 onwards, they are no longer observed.

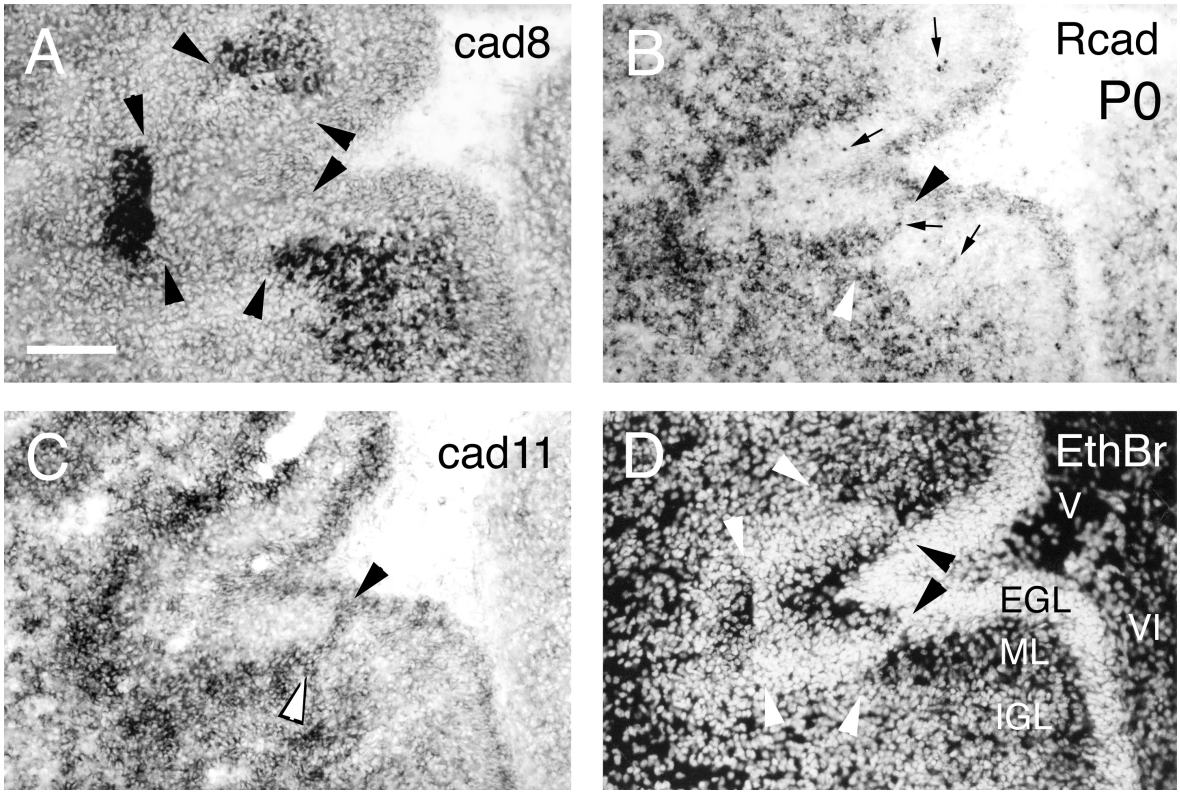

Fig. 11A-D Differential cadherin expression in the cerebellar cortex of P0 cerebellum. Adjacent transverse sections were hybridized *in situ* with anti-sense probes for cadherin-8 (*cad8* in **A**), R-cadherin (*Rcad* in **B**) and cadherin-11 (*cad11* in **C**). The section shown in **A** was counterstained with ethidium bromide (*EthBr*) for cell nuclei (**D**). The *arrowheads* point to the borders between cadherin-8-positive Purkinje cell clusters and to nuclear ribbons (raphes) in the molecular layer, respectively. The *arrows* in **B** point to single R-cadherin-expressing cells in the molecular layer. *Roman numerals* in **D** mark the cerebellar lobules. (*EGL* external granular layer; *IGL* internal granular layer; *ML* molecular layer). *Bar* 100 µm.

Relation of early-onset banding pattern of OL-protocadherin to late-onset banding pattern of zebrin II

OL-protocadherin continues to be expressed by specific Purkinje cell clusters to at least P14. A comparison of the expression patterns at P5, P7, P10, and P14 shows that the Purkinje cell clusters expressing OL-protocadherin at each stage are found at similar topological positions with respect to the evolving pattern of cerebellar foliation and growth in the mediolateral dimension (for review, see Altman and Bayer 1997). Although we could not follow the expression of OL-protocadherin at the level of individual cells, the overall impression is that the Purkinje cell domains that express OL-protocadherin at P5

retain their OL-protocadherin expression at least until P14, irrespective of variations in the level of expression and possible slight expansion of retractions of individual domains. For example, Fig. 12 depicts pairs of OL-protocadherin-immunoreactive Purkinje cell clusters at similar topological positions at P5 and P14 (Fig. 12A and B, D, and E, G and H, respectively). At P5, OL-protocadherin immunoreactivity is mostly restricted to the Purkinje cell layer. At P14, the immunoreactivity that extends into the molecular layer probably represents OL-protocadherin-positive dendrites of Purkinje cells. The positional information provided by the expression of OL-protocadherin can thus be related both to the early-onset raphe pattern and to the late-onset markers of parasagittal cerebellar banding. In this work, I compared the expression of OL-protocadherin with that of zebrin II, which is one of the best known late-onset markers (Eisenman and Hawkes 1993; Hawkes and Mascher 1994). This molecule is initially expressed by all Purkinje cells but becomes gradually restricted to subsets of Purkinje cells. In rat, the adult pattern appears from P12 onward (for review, see Hawkes and Mascher 1994). At P14, heterogeneities in the zebrin II staining, including sharp steps in staining, are found in the mouse cerebellar cortex (present results). These heterogeneities have an overall distribution that is highly similar to the pattern of zebrin II-positive and zebrin II-negative compartments in the adult mouse (Eisenmann and Hawkes 1993). According to the scheme of zebrin banding in the adult mouse proposed by these authors, I identified the corresponding bands at P14.

Figure 12 shows that several of the steps in zebrin II immunostaining at P14 (arrows in Fig. 12C, F, I) precisely coincide with borders of OL-protocadherin expression in adjacent sections (arrows in Fig. 12B, E, H). In lobules III-VIII, the OL-protocadherin-positive Purkinje cell clusters overlap extensively with the zebrin II-positive bands “P2+”, “P4+”, “P5a+”, and “P5b+” (terminology according to Eisenman and Hawkes 1993), whereas the other zebrin II-positive bands and all zebrin II-negative bands do not express OL-protocadherin. In lobules I, II, IX, and X, the OL-protocadherin immunostaining is less distinct and was difficult to relate to the zebrin II pattern. The arrows in Fig.12A, D, G indicate borders of OL-protocadherin expression in the P5 cerebellum at corresponding topological positions that, in turn, coincide with ribbons (e.g., compare Fig. 12A with Fig. 6E, F; Fig. 12D with the dorsal midline region in Fig. 6A, B; and Fig. 12G with Fig. 6C, D). Based on a comparison of several lobules at P14, I identified a correspondence between the topological positions of a ribbon at P5 and a border of zebrin II expression at P14 for the following positions (from medial to lateral): borders of midline band P1+ (Fig. 12F, ribbons marked “x_1” in Fig. 6B), medial and lateral border of band P2+ (Fig. 12F, ribbons marked “1” and “2” in Fig. 6B, respectively), lateral border of band P4b+ (Fig.

12I, ribbon marked "x_2" in Fig. 6B, C, D), lateral border of band P5b+ (Fig. 12C, ribbon marked "6" in Fig. 6B, E, F).

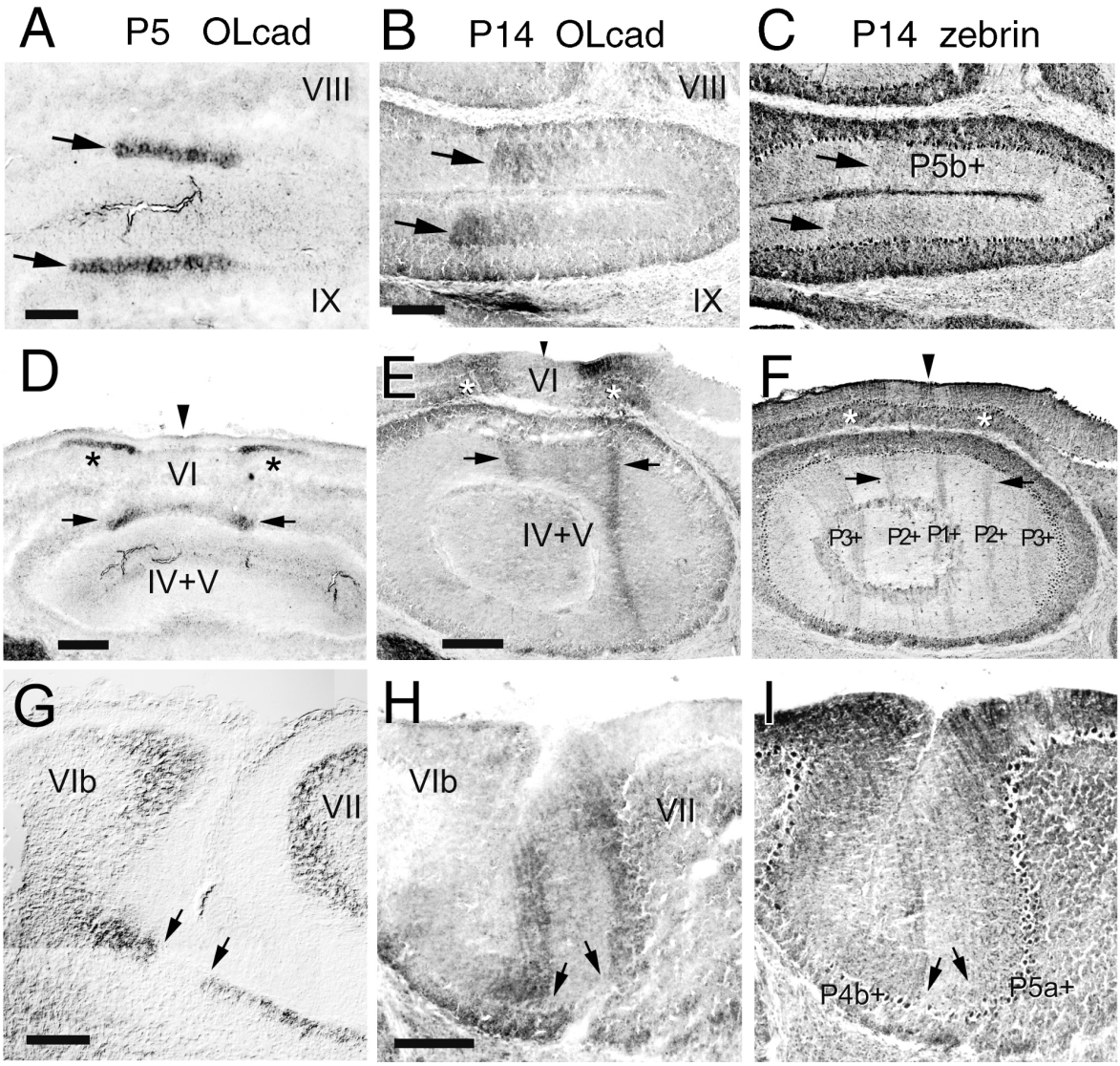

Fig. 12A-I Comparison of immunostaining results for OL-protocadherin at P5 (*Olcad* in **A**, **D**, **G**) and at P14 (**B**, **E**, **H**), and for zebrin II at P14 (*zebrin* in **C**, **F**, **I**). Each *row* shows corresponding regions of developing cerebellar cortex. The results displayed for P14 in **B** and **C**, **E** and **F**, and **H** and **I** are from adjacent sections, respectively. **A** and **G** show enlargements of the areas boxed in Fig. 6A. **D** shows an enlargement of the dorsal midline region of the section displayed in Fig. 6A. The *arrows* mark the position of borders of immunostaining. The borders marked in **A**-**C**, **D**-**F**, and **G**-**I**, respectively, are located at corresponding positions. The *arrowheads* in **D**-**F** mark the midline. The *asterisks* in **D**-**F** indicate the position of two OL-protocadherin-positive Purkinje cell clusters that are symmetrical about the midline. The letters in **C**, **F**, and **I** mark stripes in the zebrin II expression pattern, following the terminology of Eisenman and Hawkes (1993). *Roman numerals* mark the cerebellar lobules. *Bars* **A** 100 μm; **B**, **C** 200 μm; **D** 200 μm; **E**, **F** 400 μm; **G** 100 μm; **H**, **I** 200 μm.

4. DISCUSSION

The present work demonstrates parasagittal ribbons of cells in the molecular layer of mouse cerebellar cortex during the first postnatal week of development. These ribbons extend from the external granular layer into the prospective Purkinje cell layer. The ribbons are found in nearly all cerebellar lobules (Fig. 10). In the following paragraphs, I will discuss the evidence that these ribbons correspond to the granule cell raphes first described by Feirabend (1983, 1990) in the chicken, followed by a discussion of the distribution of the granule cell raphes in the mouse cerebellar cortex and their relation to early-onset and late-onset parasagittal banding patterns of cerebellar cortex.

Evidence for granule cell raphes in the mouse cerebellar cortex

The following results strongly suggest that the cell ribbons found in the postnatal mouse cerebellum in the present work are the mouse equivalent of the granule cell raphes present in chicken:

(1) Both in chicken (Arndt et al. 1998; Lin and Cepko 1998) and in mouse, the ribbons are located at the borders of distinct Purkinje cell segments, as revealed in the present work by their expression of cadherin-8, OL-protocadherin and R-cadherin (Figs. 5, 6, 7, 8, 11, 12; Korematsu and Redies 1997a; Suzuki et al. 1997; Hirano et al. 1999). Such a relationship was found in lobules III-VI (as shown in Figs. 5, 8, 11, and 12) and in most of the other lobules. Molecularly distinct Purkinje cell segments have been demonstrated previously at similar stages of mouse cerebellar development with other molecular markers (e.g., GMP-dependent protein kinase, vitamin D-dependent calcium-binding protein; Wassef et al., 1985; see reviews by Herrup and Kuemerle 1997; Oberdick et al. 1998, or other adhesion molecules, neuroplastin; Marzban et al., 2003). In the chicken, other cadherins (cadherin 6B and cadherin-7, Arndt et al. 1998; and cadherin-10, Fushimi et al. 1997) are also expressed by distinct parasagittal Purkinje cell clusters. It is at present unclear whether the expression domains of additional cadherins expressed in the mouse cerebellum (see Suzuki et al. 1997) are similarly delimited by ribbons. It is conceivable (but highly speculative) that most (if not all) ribbons will eventually be found to form boundaries of cadherin-expressing Purkinje cell clusters in both species. In the chicken, some raphes were also found inside Purkinje cell domains expressing cadherin-6B and cadherin-7 (Fig. 7A-C by Arndt et al., 1998). In the present work, raphes inside cadherin-positive Purkinje cell domains were not observed.

(2) In both chicken and mouse, the ribbons extend parasagittal over several lobules or, in some cases, over the entire cerebellar cortex. The number and spacing of the ribbons is roughly similar in mouse and in chicken (compare our Fig. 10A, B to Fig. 1A, B).

(3) In the mouse, most cells in the ribbons have a nuclear size and histological appearance in thionine stains similar to the granule cells of the innermost sheet of the external granular layer (Fig. 9C). The ribbon cells can be followed into the layer of prospective Purkinje cells (insert in Fig. 9C). Similar observations were made in the chicken (Feirabend, 1983, 1990).

(4) As in the chicken, the majority of ribbon cells express specific cadherins (e.g., cadherin-11 in mouse, see Fig. 11C; cadherin-7 and -10 in chicken, Fushimi et al. 1997; Arndt et al., 1998). The same cadherins are also expressed by the granule cells in the differentiating internal granular layer (Fig. 11C; Arndt et al., 1998). In chicken, R-cadherin is expressed only by a small subpopulation of ribbon cells that likely represent migrating interneurons (Arndt et al., 1998). Scattered R-cadherin-expressing cells are also found in the ribbons of mouse at stage P0, as well as dispersed throughout the molecular layer and the internal granular layer (Fig. 11B). Whether these cells also represent interneurons remains to be demonstrated. However, at P3, R-cadherin-expressing cells are more numerous in the ribbons and the granular layers, suggesting that at least some granule cells also begin to express this molecule at this stage of development (Fig. 7B).

(5) In both chicken and mouse, the ribbons are found at similar stages of cerebellar development (P0-P6 in mouse compared to E9-E15 in chicken). At later stages, granule cell migration through the molecular layer is more widespread and granule cell raphes are no longer observed.

(6) The ribbon cells do not express TAG-1, a marker for cells in the innermost external granular layer (data not shown; Yamamoto et al. 1986; Stottmann and Rivas 1998). Similar results were obtained in the chicken (K. Arndt and C. Redies, unpublished observations). TAG-1 expression was also reported to be absent in granule cells migrating through the molecular layer (Stottmann and Rivas 1998).

In conclusion, I propose that the ribbons found in the mouse in the present work correspond to the granule cell raphes described by Feirabend (1983) in the chicken. I therefore refer to them as *granule cell raphes* in the mouse. Lin and Cepko (1998) have previously searched for granule cell raphes in mouse but have failed to detect them. Indeed, the mouse raphes are not as prominent as those in the chicken, and it was

sometimes difficult to consistently follow an individual raphe from section to section. For this reason, I analyzed several adjacent sections before determining whether or not a raphe was present at a particular cortical cerebellar location.

Note that the cell-dense granule cell raphes in the molecular layer described in the present work are distinctly different from the cell-poor (medullary) raphes found between clusters of prospective Purkinje cells and between the deep cerebellar nuclei, first described by Korneliussen (1967, 1968). The latter type of raphes is found between clusters of prospective Purkinje cells and between the deep cerebellar nuclei at earlier embryonic stages of mammalian cerebellar development than the granule cell raphes investigated in this work. Whether the two types of "raphe" relate to each other is unclear.

The cells in the granule cell raphes do not express calbindin, a marker for Purkinje cells (Fig. 9B; Wassef et al. 1985; Iacopino et al. 1990). At the position of the raphes, gaps in calbindin staining are observed in the prospective Purkinje cell layer (Fig. 9B). Such gaps have been noticed before and were postulated to separate adhesive Purkinje cell compartments (Wassef et al. 1985). They were interpreted as being similar to the cell-poor (medullary) raphes of Korneliussen (1967, 1968; Wassef et al. 1985). Note, however, that the gaps in the layer of prospective Purkinje cells are densely packed with cells. At least some of these cells have a histological appearance similar to the cells in the granule cell raphes (Fig. 9C). Consequently, we propose that the gaps contain an extension of the raphes (see also Lin and Cepko 1998). The possibility that the gaps in calbindin immunostaining also contain calbindin-negative Purkinje cells cannot be excluded. In the mouse, the cells in the gaps represent an extension of the raphes.

The existence of granule cell migration in raphes in the mouse cerebellum was confirmed by Karam et al. (2001). Furthermore, these authors demonstrated the presence of raphes also in primate cerebellum. This finding strongly suggests that the migration of granule cells in the parasagittal raphes is an evolutionary conserved process.

Overall organization of the pattern of granule cell raphes

In the chicken, step-like changes in the expression of a large variety of different early-onset markers have been shown to coincide with raphes (Arndt et al. 1998; Lin and Cepko 1998). The raphe pattern in the chicken, and possibly also that in the mouse, can thus be interpreted as a positional reference system that represents a common topological framework underlying the patterns of many early-onset markers of parasagittal banding. Given the likely importance of the raphes pattern as an indicator of mediolateral cerebellar compartmentation, I mapped the raphe pattern over the entire cerebellar cortical surface of

the mouse at P5. The combination of raphes in the molecular layer and their extension into the gaps of calbindin immunostaining in the Purkinje layer allowed me to map the positions of the raphes (gaps) in a consistent way. Most raphes extend along several lobules in the anteroposterior dimension (Fig. 10A, B). Only about 6-8 raphes extend over almost the entire cortical surface. This number is similar to the number of mediolateral compartments previously postulated on the basis of mapping common expression boundaries for multiple parasagittal markers (Herrup and Kuemerle 1997; Oberdick et al. 1998). The precise number of the compartments in each lobule, however, is a matter of uncertainty and scientific debate, given the large number of domains that could potentially be defined by combining the partially overlapping expression patterns of multiple markers. Indeed, I found additional raphes that are likely to border additional compartments in several lobules (Fig. 10). This result is consistent with the finding that the number of parasagittal stripes or patches, e.g., of cadherin expression, varies between lobules (see Suzuki et al., 1997; Hirano et al. 1999). Moreover, in the chicken, bifurcations of individual raphes have been observed (Feirabend 1990). In my work, I did not observe such bifurcations but this failure may be due to the fact that the mouse raphes are less prominent than those in the chicken. Nevertheless, it is noteworthy that the overall number of raphes found here in the mouse at P5 approximately matches that of chicken at E14 (compare my Fig. 9A, B to Fig. 1A, B). Another marker of parasagittal banding, zebrin II, has also been reported to show an evolutionarily conserved distribution in different species (for review, see Herrup and Kuemerle 1997).

Relating positional cues from early-onset markers to those of late-onset markers of parasagittal compartmentation

One of the unsolved problems of cerebellar development is how positional cues in the early-onset pattern of parasagittal banding relate to those in the late-onset pattern. The present dissertation demonstrates that the expression of OL-protocadherin is topologically relatively invariant from P5 to at least P14, despite the considerable growth of the cerebellum during this period. Although not demonstrated at the single-cell level, individual OL-protocadherin-positive Purkinje cell clusters can be followed as distinct entities that retain their approximate position at least in some cerebellar lobules (lobules IV-IX; Fig. 12). In these lobules, the borders of OL-protocadherin expression often coincide with the position of raphes at P5. At P14, the borders of OL-protocadherin-positive Purkinje cell clusters at the same topological position, in turn, regularly coincide with heterogeneities in the expression pattern of zebrin II, a late-onset marker of

parasagittal banding (Fig. 12). This result provides indirect evidence for a spatial relationship between the early-onset banding pattern (as represented, e.g., by the raphes) and late-onset banding patterns. Specifically, the results indicate that at least some of the positional cues carried by the compartmental boundaries are shared by the two types of patterns, as previously postulated by other researchers based on other evidence (see Herrup and Kuemerle 1997). Recent results for neurogranin, which is an endogenous marker for parasagittal Purkinje cell clusters and is expressed from about E13 until P20, support a relationship between the early- and late onset patterning (Larouche at al. 2006). Whether or not exactly the same population of Purkinje cells carries these cues remains unclear, because we could not monitor individual Purkinje cells and their expression of OL-protocadherin in the vicinity of the boundaries during development. It should be noted that not all positional cues must be shared between the two types of patterns. Baader et al. (1999) reported that the ectopic expression of the transcriptional factor engrailed-2 in cerebellar Purkinje cells in mutant mice selectively disrupts late-onset patterns but not early-onset patterns. Two possible interpretations for this finding were proposed: (1) two (at least partially) distinct mediolateral boundary systems exist early and late in cerebellar development; (2) there is only one boundary system, which fails to be translated from early to late stages of development in the mutant mice (Baader et al. 1999).

Open questions on the role of the raphes in functional cerebellar patterning

The present work is descriptive and no experimental evidence for a functional role of the raphes in cerebellar patterning is provided. The following hypotheses are based on the timing of appearance of the raphes and remain speculative. Where granule cell raphes first appear in the molecular layer (around P0), the parasagittal patterning and segmentation of prospective Purkinje cells is already well advanced. Preceding the appearance of the raphes, the prospective Purkinje cell layer shows parasagittal expression of several gene regulatory proteins (see Millen et al. 1995) and of cadherins (Arndt and Redies 1996; Korematsu and Redies 1997a; Arndt and Redies 1998). The raphe pattern is therefore likely to be a consequence of primary cortical cerebellar patterning rather than its cause. At the time when the raphes appear in the postnatal cerebellum, each segment of Purkinje cells contains several layers of cadherin-expressing cells. It is conceivable that these segments are tightly adherent due to their cadherin expression and that they constitute a barrier of migrating granule cells. In this scenario, the border regions between the segments would represent a route of migration that is more permissive for granule cell migration that the Purkinje cell segments themselves. Once the granule cell raphes have

formed, they might serve to separate the Purkinje cell clusters, thus stabilizing mediolateral boundaries in the developing cerebellar cortex. A similar function of cerebellar granule cells has recently been demonstrated experimentally in Unc5h3 mutant chimerical mice with cerebellar ectopias. Here, the granule cell was interpreted to be the pioneer cell type to demarcate boundaries inside and outside the cerebellum (Goldowitz et al. 2000).

Whether the patterned migration of granule cells has an effect on the extension of parallel fibers into the molecular layer remains to be studied. Similarly open is the question of whether the transient concentration of migrating granule cells to the raphes affects intracortical connectivity patterns. Also, the precise relation of the raphe pattern to the parasagittal organization of afferent and efferent connectivity of the vertebrate cerebellum (for review, see Herrup and Kuemerle 1997; Voogd and Glickstein 1998) is unclear at present. A relation between cerebellar fiber connections and the parasagittal expression of adhesion molecules has been demonstrated for several adhesion molecules such as BEN/SCI/DM-GRASP and some cadherins (Chédotal et al. 1996; Arndt and Redies 1998; Arndt et al. 1998). Although some of the common boundaries in the parasagittal banding patterns can be related to innervation patterns (Gravel et al. 1987; Gravel and Hawkes 1990; Hawkes and Mascher 1994), experimental evidence indicates that mediolateral cerebellar patterning takes place also in the absence of afferent fiber input, based on genetic mechanisms that are partially intrinsic to cerebellar tissue (Wassef et al. 1990; Oberdick et al. 1993; Chédotal et al. 1996).

5. ABSTRACT

The cerebellar cortex of many vertebrates shows a striking parasagittal compartmentation that is thought to play a role in the establishment and maintenance of functional cerebellar connectivity.

Here, I demonstrate the existence of multiple parasagittal raphes of cells in the molecular layer of the developing cerebellar cortex of postnatal mouse.

The histological appearance and immunostaining profile of the raphe cells suggest that they are migrating granule cells. I therefore conclude that the granule cell raphes previously described in birds also exist in a mammalian species. The raphes in mouse are visible on nuclear stains from around birth to postnatal day 6 and are frequently found at the boundaries of Purkinje cell segments that differentially express cadherins ("early-onset" parasagittal banding pattern). A similar relation between the raphe pattern and various markers for the early-onset banding pattern has been found in the chicken cerebellum. One of the cadherins mapped in the present study (OL-protocadherin) continues to be expressed in specific Purkinje cell segments until at least postnatal day 14. At this stage of development, the borders of the OL-protocadherin-positive Purkinje cell segments coincide with the borders of Purkinje cell segments that express zebrin II, a marker for the "late-onset" parasagittal banding pattern which persists in the adult cerebellum.

These findings demonstrate that the early-onset banding pattern, as reflected in the complementary arrangement of raphes/Purkinje cell segments, and the late-onset pattern of zebrin II expression share at least some positional cues during development.

6. REFERENCES

1. Altman, J., Bayer, S.A. (1997):
Development of the cerebellar system.
CRC Press, Boca Raton, FL

2. Amagai, M., Klaus-Kovtun, V., Stanley, J. R. (1991):
Autoantibodies against a novel epithelial cadherin in pemphigus vulgaris, a disease of cell adhesion.
Cell 67, 869-877.

3. Arends, J.J.A., Zeigler, H.P. (1991):
Organization of the cerebellum in the pigeon (*Columba livia*). I. Corticonuclear and corticovestibular connections.
J. Comp. Neurol. 306, 221-244.

4. Arndt, K., Redies, C. (1996):
Restricted expression of R-cadherin by brain nuclei and neural circuits of the developing chicken brain.
J. Comp. Neurol. 373, 373-399.

5. Arndt, K., Redies, C. (1998):
Development of cadherin-defined parasagittal subdivisions in the embryonic chicken cerebellum.
J. Comp. Neurol. 401, 367-381.

6. Arndt, K., Nakagawa, S, Takeichi, M., Redies, C. (1998):
Cadheirn-defined segments and parasagittal cell ribbons in the developing chicken cerebellum.
Mol. Cell Neurosci. 10, 211-228.

7. Baader, S.L., Vogel, M.W., Sanlioglu, S., Zhang, X., Oberdick, J. (1999):
Selective disruption of “late-onset” sagittal banding patterns by ectopic expression of engrailed-2 in cerebellar Purkinje cells.
J. Neurosci. 19, 5370-5379.

8. Bähr, M., Frotscher, M., Küker, W. (2003):
Duus` neurologisch-topische Diagnostik. 8th edition.
Stuttgart: Thieme.

9. Boegman, R., Parent, A., Hawkes, R. (1988):
Zonation in the rat cerebellar cortex: Patches of high acetylcholinesterase activity in the granular layer are congruent with Purkinje cell compartments.
Brain. Res. 448, 237-251.

10. Cepek, K.L., Shaw, S.K., Parker, C.M., Russel, G.J., Morrow, J.S., Rimm, D.L., Brenner, M.B. (1994):
Adhesion between epithelial cells and T-lymphocytes mediated by E-cadherin and the aEb7 integrin.
Nature 372, 190-193.

11. Chédotal, A., Pourquié, O., Ezan, F., Clemente, H.S., Sotelo, C. (1996):
BEN as a presumptive target recognition molecule during the development of the olivocerebellar system.
J. Neurosci. 16, 3296-3310.

12. Cowley, G.P., Smith, M.E. (1996):
Cadherin expression in melanocytic naevi and malignant melanomas.
J. Pathol. 179, 183-187.

13. Eisenmann, L.M., Hawkes, R. (1990):
5`-nucleotidase and the mabQ113 antigen share a common distribution in the cerebellar cortex of the mouse.
Neuroscience 31, 231-235.

14. Eisenman, L.M., Hawkes, R. (1993):
Antigenic compartmentation in the mouse cerebellar cortex: zebrin and HNK-1 reveal a complex, overlapping molecular topography.
J. Comp. Neurol. 335, 586-605.

15. Feirabend, H.K.P. (1983):
Anatomy and development of longitudinal patterns in the architecture of the cerebellum of the White Leghorn (*Gallus domesticus*).
Ph thesis, Rijkuniversiteit te Leiden.

16. Feirabend, H.K.P. (1990):
Development of longitudinal patterns in the cerebellum of the chicken (*Gallus domesticus*): a cytoarchitectural study on the genesis of cerebellar modules.
Eur. J. Morphol. 28, 169-223.

17. Furley, A.J., Morton, S.B., Manalo, D., Karagogeos, D., Dodd, J., Jessell, T.M. (1990):
The axonal glycoprotein TAG-1 is an immunoglobulin superfamily member with neurite outhgrowth-promoting activity.
Cell 61, 157-170.

18. Fushimi, D., Arndt, K., Takeichi, M., Redies, C. (1997):
Cloning and expression analysis of cadherin-10 in the CNS of the chicken embryo.
Dev. Dyn. 209, 269-285.

19. Goldowitz, D., Hamre, K. (1998):
The cells and molecules that make a cerebellum.
Trends Neurosci. 21, 375-382.

20. Goldowitz, D., Hamre, K.M., Przyborski, S.A., Ackerman S.L. (2000):
Granule cells and cerebellar boundaries: analysis of unc5h3 mutant chimeras.
J. Neurosci. 20, 4129-4137.

21. Gravel, C., Eisenman, L.M., Sassaville, R., Hawkes, R. (1987):
Parasagittal organization of the rat cerebellar cortex: direct correlation between antigenic Purkinje cell bands revealed by mabQ113 and the organization of the olivocerebellar projection.
J. Comp. Neurol. 265, 294-310.

22. Gravel, C., Hawkes, R. (1990):
Parasagittal organization of the rat cerebellar cortex: direct comparison of Purkinje cell compartments and the organization of spinocerebellar projection.
J. Comp. Neurol. 291, 79-102.

23. Groenewegen, H.J., Voogd, J. (1976):
The parasagittal zonation within the olivocerebellar projection. I. Climbing fiber distribution in the vermis of cat cerebellum.
J. Comp. Neurol. 174, 417-488.

24. Hashimoto, M., Mikoshiba, K., (2003):
Mediolateral compartmentalization of the cerebellum is determined on the ”birth date“ of Purkinje cells.
J. Neurosci. 23, 11342-11351.

25. Hatten, M.E. (1993):
The role of migration in central nervous system neuronal development.
Curr. Opin. Neurobiol. 3, 38-44.

26. Hawkes, R., Leclerc, N. (1987):
Antigenic map of the rat cerebellar cortex: the distribution of parasagittal bands as revealed by monoclonal anti-Purkinje cell antibody mabQ113.
J. Comp. Neurol. 256, 29-41.

27. Hawkes, R., Mascher, C. (1994):
The development of molecular compartmentation in the cerebellar cortex.
Acta. Anat. (Basel) 151, 139-149.

28. Herrup, K., Kuemerle, B. (1997):
The compartmentalization of the cerebellum.
Annu. Rev. Neurosci. 20, 61-90.

29. Hirano, S., Yan, Q., Suzuki, S.T., (1999):
Expression of a novel protocadherin, OL-protocadherin, in a subset of functional systems of the developing mouse brain.
J. Neurosci. 19, 995-1005.

30. Iacopino, A.M., Rhoten, W.B., Christakos, S. (1990):
Calcium binding protein (calbindin-D28k) gene expression in the developing and aging mouse cerebellum.
Mol. Brain Res. 8, 283-290.

31. Ito, M. (1993):
New concepts in cerebellar function.
Rev. Neurol., 149, 596-599.

32. Karam, S., Kim, Y., Bothwell, M. (2001):
Granule cells migrate within raphes in the developing cerebellum: An evolutionarily conserved morphogenic event.
J. Comp. Neurol. 440, 127-135.

33. Korematsu, K., Redies, C. (1997a):
Expression of cadherin-8 mRNA in the developing mouse central nervous system.
J. Comp. Neurol. 387, 291-306.

34. Korematsu, K., Redies, C. (1997b):
Restricted expression of cadherin-8 in segmental and functional subdivisions of the embryonic mouse brain.
Dev. Dyn. 208, 178-189.

35. Korneliussen, H.K., (1967):
Cerebellar corticogenesis in Cetaca, with special reference to regional variations.
J. Hirnforsch. 9, 151-185.

36. Korneliussen, H.K., (1968):
On the ontogenetic development of the cerebellum (nuclei, fissures, and cortex of the rat, with special reference to regional variations in corticogenesis).
J. Hirnforsch. 10, 379-412.

37. Larouche, M., Che, P., Hawkes, R. (2006):
Neurogranin expression identifies a noval array of Purkinje cell parasagittal stripes during mouse cerebellar development.
J. Comp. Neurol. 494, 215-227.

38. Larouche, M., Hawkes, R. (2006):
From clusters to stripes: The developmental origins of adult cerebellar compartmentations.
The Cerebellum. 5, 77-88.

39. Larsell, O., (1952):
The morphogenesis and adult pattern of the lobules and fissures of the cerebellum of the white rat.
J. Comp. Neurol. 97, 281-356.

40. Leclerc, N., Doré, L., Parent, A., Hawkes, R. (1990):
The compartmentalization of the monkey and rat cerebellar cortex: Zebrin I and cytochrome oxidase.
Brain. Res. 506, 70-78.

41. Lin, J.C., Cepko, C.L. (1998):
Granule cell raphes and parasagittal domains of Purkinje cells: complementary patterns in the developing chick cerebellum.
J. Neurosci. 18, 9342-9353.

42. Luo, J., Treubert-Zimmermann, U., Redies, C. (2004):
Cadherins guide migrating Purkinje cells to specific parasagittal domains during cerebellar development.
Mol. Cell Neurosci. 25, 138-152.

43. Marzban, H., Khanzada, U., Shabir, S., Hawkes, R., Langnaese, K., Smalla, K.H., Bockers, T.M., Gundelfinger, E.D., Gordon-Weeks, P.R., Beesley, P.W. (2003): Expression of the immunoglobulin superfamily neuroplastin adhesion molecules in adult and developing mouse cerebellum and their localization to parasagittal stripes. J. Comp. Neurol. 9, 286-301.

44. Mathis, L., Bonnerot, C., Puelles, L., Nicolas, J.F. (1997): Retrospective clonal analysis of the cerebellum using genetic laacZ/lacZ mouse mosaics. Development 124, 4089-4104.

45. Millen, K.J., Hui, C.C., Joyner, A.L. (1995): A role for En-2 and other murine homologues of *Drosophila* segment polarity genes in regulating positional information in the developing cerebellum. Development 121, 3935-3945.

46. Oberdick, J., Schilling, K., Smeyne, R.J., Corbin, J.G., Bocchiaro, C., Morgan, J.I., (1993): Control of segment-like patterns of gene expression in the mouse cerebellum. Neuron 10, 1007-1018.

47. Oberdick, J., Baader, S.L., Schilling, K. (1998): From zebra stripes to postal zones: deciphering patterns of gene expression in the cerebellum. Trends Neurosci. 21, 383-390.

48. Overduin, M., Harvey, T.S., Bagby, S., Tong, K.I., Yau, P., Takeichi, M., Ikura, M., (1995): Solution structure of the epithelial cadherin domain responsible for selective cell adhesion. Science 267, 386-389.

49. Rakic, P. (1971):
Neuron-glia relationship during granule cell migration in developing cerebellar cortex. A Golgi and electromicroscopic study in *Macaccus rhesus*.
J. Comp. Neurol. 141, 283-312.

50. Redies, C. (2000):
Cadherins in the central nervous system.
Prog. Neurobiol. 61, 611-648.

51. Redies, C., Vanhalst, K., van Roy, F. (2005):
δ-Protocadherins: unique structures and functions.
Cell. Mol. Life Sci. 62, 2840-2852.

52. Rubinek, T., Yu, R., Hadani, M., Barkai, G., Nass, D., Melmed, S., Shimon, I. (2003):
The cell adhesion molecules N-cadherin and neural cell adhesion molecule regulate human growth hormone: a novel mechanism for regulating pituitary hormone secretion.
J. Clin. Endocrinol. Metab. 88, 3724-3730.

53. Sarna, J.R., Marzban, H., Watanabe, M., Hawkes, R. (2006):
Complementary stripes of phospholipase Cbeta3 and Cbeta4 expression by Purkinje cell subsets in the mouse cerebellum.
J. Comp. Neurol. 496, 303-313.

54. Shapiro, L., Fannon, A.M., Kwong, P.D., Thompson, A., Lehmann, M.S., Grübel, G., Legrand, J.-F., Als-Nielsen, J., Colman, D.R., Hendrickson, W.A., (1995):
Structural basis of cell-cell adhesion by cadherins.
Nature 374, 327-337.

55. Smith, S.H., Goldschmidt, M.H., McManus, P.M. (2002):
A comparative review of melanocytic neoplasms.
Vet. Pathol. 39, 651-671.

56. Sotelo C., Alvarado-Mallart, R.-M., Frain, M., Vernet, M. (1994):
Molecular plasticity of adult Bergmann fibers is associated with radial migration of grafted Purkinje cells.
J. Neurosci. 14, 124-133.

57. Stottmann, R.W., Rivas, R.J. (1998):
Distribution of TAG-1 and synaptophysin in the developing cerebellar cortex: relationship to Purkinje cell dendritic development.
J. Comp. Neurol. 395, 121-135.

58. Sugihara, I. (2006):
Organization and remodeling of the olivocerebellar climbing fiber projection.
Cerebellum 5, 15-22.

59. Suzuki, S.C., Inoue, T., Kimura, Y., Tanaka, T., Takeichi, M. (1997):
Neuronal circuits are subdivided by differential expression of type-II classic cadherins in postnatal mouse brains.
Mol. Cell Neurosci. 9, 433-447.

60. Takeichi, M., Atsumi, T., Yoshida, C., Uno, K., Okada, T.S. (1981):
Selective adhesion of embryonal carcinoma cells and differentiated cells by Ca^{2+}-dependent sites.
Dev. Biol. 87, 340-350.

61. Takeichi, M. (1988):
The cadherins: cell-cell adhesion molecules controlling animal morphogenesis.
Development 102, 639-655.

62. Trepel, M. (1995):
Neuroanatomie: Struktur und Funktion.
München, Wien, Baltimore: Urban und Schwarzenberg.

63. Voogd, J., Glickstein, M. (1998):
The anatomy of the cerebellum.
Trends Neurosci. 21, 370-375.

64. Wassef, M., Zanetta, J.P., Brehier, A., Sotelo, C. (1985):
Transient biochemical compartmentalization of Purkinje cells during early cerebellar development.
Dev. Biol. 111, 129-137.

65. Wassef, M., Cholley, B., Heizmann, C.W., Sotelo, C. (1992):
Development of the olivocerebellar projection in the rat. II. Matching of the developmental compartmentations of the cerebellum and the inferior olive through the projection map.
J. Comp. Neurol. 323, 537-550.

66. Yamamoto, M., Boyer, A.M., Crandall, J.E., Edwards, M., Tanaka, H., (1986):
Distribution of stage-specific neurite-associated proteins in the developing murine nervous system recognized by a monoclonal antibody.
J. Neurosci. 6, 3576-3594.

7. LIST OF ILLUSTRATIONS

8. LIST OF ABBREVIATIONS

BCIP	5-bromo-4-chloro-3-indolylphosphate-p-toluidin salt
CNS	central nervous system
Cy3	indocarbocyanine dye
DAB	3-3`diaminobenzidinetetrahydrochloride
DEPC	diethylpyrocarbonate
E	embryonic day
E-cadherin	epithelial cadherin
EDTA	ethylendiamine tetra acetic acid
EGL	external granular layer
FL	flocculus
HBSS	HEPES-buffered salt solution
IGL	internal granular layer
ISH	in situ hybridization
NBT	nitroblue tetrazolium salt
N-cadherin	neural cadherin
P	postnatal day
P-cadherin	placental cadherin
PBS	phosphate-buffered saline
PFL	paraflocculus
R-cadherin	retinal cadherin
SSC	citrate-buffered salt solution
TBS	Tris-buffered saline

ACKNOWLEDGMENTS

- Special thanks to Prof. Dr. Dr. Ch. Redies for the supervision of this dissertation and his generous time and commitment. For his patience and helpfulness in the solution of difficult questions. Throughout my doctoral work he encouraged me to develop independent thinking and research skills.

I am also very grateful for having an exceptional doctoral committee and wish to thank:

- Dr. K. Obst-Pernberg kindly introduced me to the different techniques used in the present work.
- Dr. Ullrich Treubert-Zimmermann for inspiring discussions.
- U. Jonetat and U. Laub for expert technical assistance.
- D. Kittel, R. Düchting and P. Babioch for help with photography.
- Dr. S. Hirano and Dr. S. T. Suzuki provided an unpublished antibody against mouse OL-protocadherin.
- Y. Kimura, S. Kozlov, H. Matsunami and M. Takeichi for cDNAs.
- I thank my parents, my brother and all of my friends for their continued support.

- This work was supported by a grant from the German Research Council (Re 616/4-1).

10. CURRICULUM VITAE

Personal data:	Robert Luckner
	Recklinghausen
	born May 03, 1975
	in Bytom (Poland)

Education:

1982-1988	Basic Primary School, Rokitnica (Poland)
1988-1995	Gymnasium Johanneum, Ostbevern
1995	Final secondary-school examination (“Abitur”)

Alternative Civilian Service:

1995-1996	Städtisches Klinikum, Duisburg

Medical Studies:

1996-2003	Medical studies at the University of Essen School of Medicine
2003	National Board Examination (Staatsexamen)

Occupational activity:

Jan. 2004- Sep. 2005	Department of Neurosurgery, evangelisches Krankenhaus in Bielefeld
Since Oct. 2005	Department of Neurosurgery, Knappschaftskrankenhaus in Recklinghausen